NEW ENERGY FOR INDUSTRY

Industry4Redispatch (I4RD)

Deliverable 5.2

Specification of the TSO-DSO interaction process

AUTHORS

Daniel-Leon Schultis*	**daniel-leon.schultis@ait.ac.at**	**AIT Austrian Institute of Technology GmbH**
Sawsan Henein	**sawsan.henein@ait.ac.at**	**AIT Austrian Institute of Technology GmbH**
Felix Hembach	**felix.hembach@apg.at**	**Austrian Power Grid AG**
Thomas Fabian	**thomas.fabian@siemens.at**	**Siemens AG Österreich**
Sophie Knöttner	**sophie.knoettner@ait.ac.at**	**AIT Austrian Institute of Technology GmbH**

* Corresponding author

PROJECT MANAGEMENT

AIT – Tara Esterl
+43 664 8157 810
Tara.esterl@ait.ac.at

This project Industry4Redispatch (I4RD, FFG #886469) is supported with the funds from the Climate and Energy Fund and implemented in the framework of the RTI-initiative “Flagship region Energy”.

Document control information	
Title	D5.2 Specification of the TSO-DSO interaction process
Dissemination Level	☐ **CO** Confidential, only for members of the consortium ☐ **RE** Restricted to a group specified by the consortium ☐ **PP** Restricted to other programme participants (NEFI) ☒ **PU** Public
Status	☐ Draft ☒ WP Manager accepted ☒ Co-ordinator accepted

TABLE OF CONTENTS

LIST OF FIGURES

LIST OF TABLES

LIST OF ABBREVIATIONS

API	Application programming interface
COA	Common observability area
DS	Distribution system
DSO	Distribution system operator
EDI	Electronic Data Interchange
HV	High voltage
I4RD	Industry4Redispatch
MV	Medium voltage
REST	Representational State Transfer
TSO	Transmission system operator

LIST OF VARIABLES

The variables are listed separately for scalars, vectors, and matrices. Vectors and matrices are indicated by bold fonts in this document.

Scalars:

L	Number of loads in the regarded system portion
N	Number of critical nodes in the regarded system portion
B	Number of critical branches in the regarded system portion
ρ	Number of on-load tap changers in the regarded system portion
T	Number of time points in the regarded time horizon
F	Number of bids submitted by industries connected to the regarded system portion
M	Number of contingency cases relevant to ensure (n-1) security
$\tilde{P}_{m,t,l}^{\mathrm{base}}$	Baseline active power contribution of load l at time point t for contingency case m
$\tilde{Q}_{m,t,l}^{\mathrm{base}}$	Baseline reactive power contribution of load l at time point t for contingency case m
$U_{m,t,n}^{\mathrm{base}}$	Baseline voltage magnitude of node n at time point t for contingency case m
$\lambda_{m,t,b}^{\mathrm{base}}$	Baseline loading of branch b at time point t for contingency case m
$P_{m,t,b}^{\mathrm{base}}$	Baseline active power flow through branch b at time point t for contingency case m
$\theta_{m,t,\sigma}^{\mathrm{base}}$	Baseline tap position of tap changer σ at time point t for contingency case m
$\Delta\tilde{P}_{m,t,l}$	Active power changes of load l at time point t for contingency case m
$\Delta\tilde{Q}_{m,t,l}$	Reactive power changes of load l at time point t for contingency case m
$\Delta\tilde{P}_{t,f}^{\mathrm{bid}}$	Active power changes offered by bid f at time point t
$\Delta\tilde{Q}_{t,f}^{\mathrm{bid}}$	Reactive power changes offered by bid f at time point t
$\Delta\tilde{P}_{t}^{\mathrm{DSO/TSO}}$	Total redispatch power of regarded bid set at time point t
$\cos(\varphi_f)$	Power factor of bid f
C_f^{bid}	Cost of bid f
ε_{f_1,f_2}	XOR conflict indicator between bids f_1 and f_2
x_f	Boolean decision variable, indicating whether bid f is included in the regarded bid set or not
$C^{\mathrm{bid\ set}}$	Cost of the regarded bid set

Vectors:

$\tilde{\boldsymbol{P}}_{m,t}^{\mathrm{base}}$	Baseline active power contributions of all loads at time point t for contingency case m
$\tilde{\boldsymbol{Q}}_{m,t}^{\mathrm{base}}$	Baseline reactive power contributions of all loads at time point t for contingency case m
$\boldsymbol{U}_{m,t}^{\mathrm{base}}$	Baseline voltage magnitudes of all nodes at time point t for contingency case m
$\boldsymbol{\lambda}_{m,t}^{\mathrm{base}}$	Baseline loadings of all branches at time point t for contingency case m
$\boldsymbol{P}_{m,t}^{\mathrm{base}}$	Baseline active power flows through all branches at time point t for contingency case m
$\boldsymbol{\theta}_{m,t}^{\mathrm{base}}$	Baseline tap positions of all on-load tap changers at time point t for contingency case m
$\Delta\tilde{\boldsymbol{P}}_{m,t}$	Active power changes of all loads at time point t for contingency case m

$\Delta\widetilde{\boldsymbol{Q}}_{m,t}$	Reactive power changes of all loads at time point t for contingency case m
$\boldsymbol{U}_{m,t}^{\text{dev}}$	Deviated voltage magnitudes of all nodes at time point t for contingency case m
$\boldsymbol{\lambda}_{m,t}^{\text{dev}}$	Deviated loadings of all branches at time point t for contingency case m
$\boldsymbol{P}_{m,t}^{\text{dev}}$	Deviated active power flows through all branches at time point t for contingency case m
$\boldsymbol{\theta}_{m,t}^{\text{dev}}$	Deviated tap positions of all on-load tap changers at time point t for contingency case m
$\boldsymbol{U}_{m,t}^{\text{dev,est}}$	Estimated values of the deviated voltage magnitudes of all nodes at time point t for contingency case m
$\boldsymbol{\lambda}_{m,t}^{\text{dev,est}}$	Estimated values of the deviated loadings of all branches at time point t for contingency case m
$\boldsymbol{U}_{t}^{\text{dev,act}}$	Actual/simulated values of the deviated voltage magnitudes of all nodes at time point t
$\boldsymbol{\lambda}_{t}^{\text{dev,act}}$	Actual/simulated values of the deviated loadings of all branches at time point t
$\Delta\boldsymbol{U}_{m,t}$	Impact of load changes on the voltage magnitudes of all nodes at time point t for contingency case m
$\Delta\boldsymbol{\lambda}_{m,t}$	Impact of load changes on the loadings of all branches at time point t for contingency case m
$\Delta\boldsymbol{\theta}_{m,t}$	Impact of load changes on the tap positions of all on-load tap changers at time point t for contingency case m
$\Delta\boldsymbol{U}_{m,t}^{\text{est}}$	Estimated impact of load changes on the voltage magnitudes of all nodes at time point t for contingency case m
$\Delta\boldsymbol{\lambda}_{m,t}^{\text{est}}$	Estimated impact of load changes on the loadings of all branches at time point t for contingency case m
$\Delta\boldsymbol{P}_{m,t}^{\text{est}}$	Estimated impact of load changes on the active power flows through all branches at time point t for contingency case m
$\Delta\boldsymbol{U}_{t}^{\text{act}}$	Actual/simulated impact of load changes on the voltage magnitudes of all nodes at time point t
$\Delta\boldsymbol{\lambda}_{t}^{\text{act}}$	Actual/simulated impact of load changes on the loadings of all branches at time point t
$\Delta\boldsymbol{P}_{t}^{\text{act}}$	Actual/simulated impact of load changes on the active power flows through all branches at time point t
$\Delta\boldsymbol{P}_{m,t}$	Impact of load changes on the active power flows through all branches at time point t for contingency case m
$\Delta\widetilde{\boldsymbol{P}}_{t}^{\text{dir}}$	Direct active power changes of all loads at time point t
$\Delta\widetilde{\boldsymbol{Q}}_{t}^{\text{dir}}$	Direct reactive power changes of all loads at time point t
$\Delta\widetilde{\boldsymbol{P}}_{m,t}^{\text{ind}}$	Indirect active power changes of all loads at time point t for contingency case m
$\Delta\widetilde{\boldsymbol{Q}}_{m,t}^{\text{ind}}$	Indirect reactive power changes of all loads at time point t for contingency case m
$\Delta\widetilde{\boldsymbol{P}}_{f}^{\text{bid}}$	Active power changes offered by bid f for all time points
$\Delta\widetilde{\boldsymbol{Q}}_{f}^{\text{bid}}$	Reactive power changes offered by bid f for all time points
$\Delta\widetilde{\boldsymbol{P}}_{t}^{\text{bid}}$	Active power changes offered by all bids at time point t
$\Delta\widetilde{\boldsymbol{Q}}_{t}^{\text{bid}}$	Reactive power changes offered by all bids at time point t
$\Delta\widetilde{\boldsymbol{P}}_{t}^{\text{bid set}}$	Bid set vector, including the active power changes offered by the regarded bid set at time point t
$\Delta\widetilde{\boldsymbol{Q}}_{t}^{\text{bid set}}$	Bid set vector, including the reactive power changes offered by the regarded bid set at time point t
$\Delta\widetilde{\boldsymbol{P}}_{t}^{\text{dir}}$	Direct load change vector, including the direct active power changes of all loads at time point t
$\Delta\widetilde{\boldsymbol{Q}}_{t}^{\text{dir}}$	Direct load change vector, including the direct reactive power changes of all loads at time point t
$\boldsymbol{C}^{\text{bids}}$	Costs of all submitted bids
$\boldsymbol{x}$	Boolean decision vector, indicating which bids are included in the regarded bid set
$\boldsymbol{\lambda}^{\max}$	Upper loading limits of all branches
$\boldsymbol{U}^{\max}$	Upper voltage limits of all nodes

$\boldsymbol{U}^{\min}$	Lower voltage limits of all nodes
$\Delta\boldsymbol{U}_t^{\mathrm{err}}$	Absolute estimation errors of all node voltage magnitudes at time point t
$\Delta\boldsymbol{\lambda}_t^{\mathrm{err}}$	Absolute estimation errors of all branch loadings at time point t
$\Delta\boldsymbol{P}_t^{\mathrm{err}}$	Absolute estimation errors of all branch active power flows at time point t

Matrices:

$\boldsymbol{\varepsilon}$	XOR linkage matrix, indicating XOR conflicts between the submitted bids
$\boldsymbol{y}$	Bid allocation matrix, indicating which bid is submitted by which load
$\boldsymbol{J}_{m,t}^{U/P}$	Sensitivity matrix, including the sensitivities of all node voltage magnitudes with respect to the active power changes of all loads for contingency case m
$\boldsymbol{J}_{m,t}^{U/Q}$	Sensitivity matrix, including the sensitivities of all node voltage magnitudes with respect to the reactive power changes of all loads for contingency case m
$\boldsymbol{J}_{m,t}^{U/\theta}$	Sensitivity matrix, including the sensitivities of all node voltage magnitudes with respect to the tap position changes of all on-load tap changers for contingency case m
$\boldsymbol{J}_{m,t}^{\lambda/P}$	Sensitivity matrix, including the sensitivities of all branch loadings with respect to the active power changes of all loads for contingency case m
$\boldsymbol{J}_{m,t}^{\lambda/Q}$	Sensitivity matrix, including the sensitivities of all branch loadings with respect to the reactive power changes of all loads for contingency case m
$\boldsymbol{J}_{m,t}^{\lambda/\theta}$	Sensitivity matrix, including the sensitivities of all branch loadings with respect to the tap position changes of all on-load tap changers for contingency case m
$\boldsymbol{J}_{m,t}^{P/P}$	Sensitivity matrix, including the sensitivities of all branch active power flows with respect to the active power changes of all loads for contingency case m
$\boldsymbol{J}_{m,t}^{P/Q}$	Sensitivity matrix, including the sensitivities of all branch active power flows with respect to the reactive power changes of all loads for contingency case m
$\boldsymbol{J}_{m,t}^{P/\theta}$	Sensitivity matrix, including the sensitivities of all branch active power flows with respect to the tap position changes of all on-load tap changers for contingency case m

EXECUTIVE SUMMARY

Utilizing distributed flexibilities, such as flexibility bids of industrial customers, for redispatch at the transmission level requires a close interaction of distribution (DSO) and transmission system operators (TSO). This interaction shall avoid that the simultaneous activation of numerous flexibilities on request of the TSO causes violations of the operational distribution system (DS) limits (loading and voltage). This deliverable presents and pre-validates the DSO/TSO interaction process developed in the Industry4Redispatch (I4RD) project and overviews the simulation environment developed for process pre-validation.

According to the requirements specified in D5.1, the planned DSO/TSO interaction requires a DS model that includes low amounts of confidential data, enables quick computation, and allows validating compliance with the operational distribution network limits after bid set activation. A simplified linearized DS model is developed and analysed within the I4RD project to meet these requirements. Its parameters encompass exclusively the baseline state (loading and voltage values) of critical network elements and some sensitivity values, thus including much less confidential data as the complete AC load flow model. However, distribution systems contain several non-linearities, such as network- and control-related ones, which are not captured by the developed model.

The planned DSO/TSO interaction process is designed to promote transparency and practicability (quick computation and preserved privacy of DSOs) at the cost of accuracy. The simplified DS model is used to formulate an optimization problem for the identification of the pareto optimal bid sets, i.e., bid combinations with low cost and high power that do not violate any distribution network constraints at the high (HV) and medium voltage (MV) levels. A genetic algorithm (NSGA2) solves the formulated problem on a central redispatch platform. Redispatch bids are considered as 24h timeseries to enable the consideration of catch-up and anticipatory effects (see D3.3). The pareto optimal bid sets are forwarded to the TSO who selects the most suitable one to solve the congestion in its own grid.

A simulation environment is developed to enable the analysis of the simplified DS model, the pre-validation of the designed DSO/TSO interaction process, and the scalability analysis conducted in WP8. It is set up in DIgSILENT Power Factory and Python and contains several functionalities that facilitate three major tasks: scenario definition, process simulation, and process / model evaluation. Particular attention is paid to developing efficient code with low memory requirements and computing times to cope with the immense number of possible bid sets (*N* bids → 2^N bid sets, if no XOR links exist) in the scalability analysis.

A simulation study is conducted to check whether the simplified DS model is a suitable basis for problem formulation and whether the NSGA2 algorithm reliably finds the pareto front of the formulated problem. Results indicate that the linearized model accurately estimates branch loadings and active power flows but reveal serious problems in voltage estimation. Consequently, the derived optimization problem formulation does not guarantee the rejection of all infeasible bid sets when the actual voltage limits of the distribution network are used. Applying tightened limits removes all false approvals but increases the number of false rejections, which ultimately reduces the available redispatch power and increases the associated costs. In the investigated example, the NSGA2 algorithm correctly identifies the pareto front of the formulated optimization problem when no margins are applied, but when margins are applied, it does not find any solution. However, the simulation of a single scenario is not sufficient to conclusively evaluate the applicability of the planned DSO/TSO interaction process. Therefore, a comprehensive scalability analysis will be conducted in WP8 of this project.

1. Introduction

1.1. Purpose of the document

The final specification of the planned DSO/TSO interaction process (Task 5.5), which ensures that the activation of industrial flexibilities on request of the TSO does not lead to violations of the operational distribution network limits at the HV and MV levels, is documented. The simulation environment developed for the conceptual implementation and pre-validation of the process, is overviewed, and the pre-validation results are discussed (Task 5.4). Therefore, this document provides a detailed process description and provides insights into the performance of the process for specific test cases.

1.2. Relation to other project activities

Figure 1 shows that Tasks 5.4 and 5.5, which are covered by this deliverable, build upon Task 5.3 (initial process specification, documented in D5.1), and WP4 (schedules and bids from industrial customers). The interaction between T5.4 and T5.5 is an iterative process that promotes continuous improvements through repeated testing and adaptation of algorithms. The detailed process specification and its pre-validation lay the foundation for the cost-benefit-analysis from the DSO-perspective (WP7, see D7.1), for the scalability analysis (WP8), and for the proof-of-concept (WP9), and provide valuable insights for the development of guidelines for the DSO/TSO interaction (WP10). The process design is closely coordinated with the related working groups of Österreichs Energie.

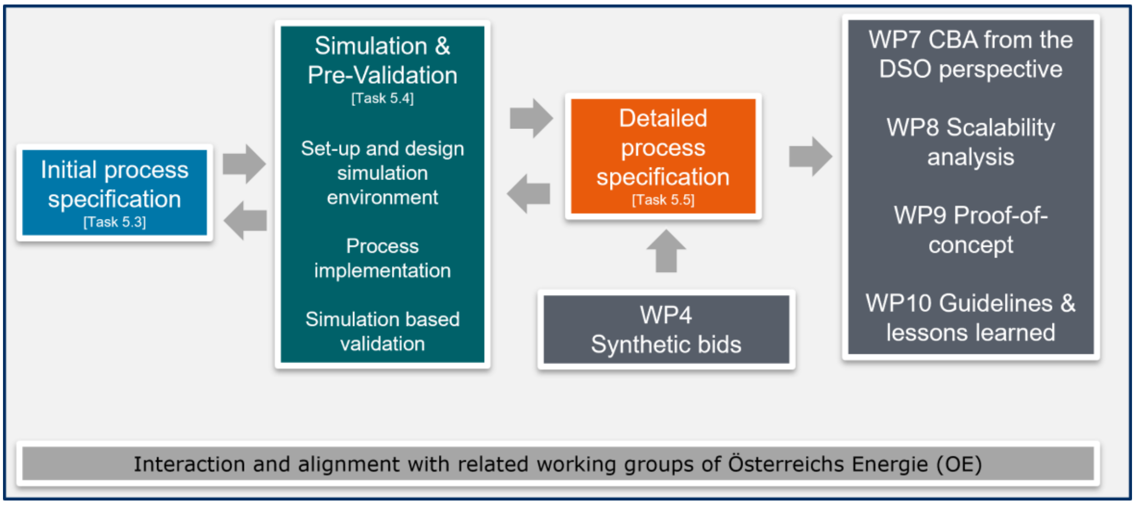

Figure 1: Interaction and alignment with related work packages and tasks.

1.3. Structure of the document

Section 2 describes the simplified DS model, which constitutes the foundation of the planned DSO/TSO interaction process. The final interaction process is documented in section 3, and section 4 presents the developed simulation environment and results. Conclusions are drawn in section 5.

2. The simplified distribution system model

The DSO/TSO interaction process described and analyzed in section 3 requires a distribution system model that

- includes low amounts of confidential data, such as topological information and line/transformer parameters, to preserve the privacy of DSOs (the model is provided by the DSO to an external platform),
- reduces computation effort to enable quick process execution,
- allows validating the feasibility of bid sets, i.e., compliance with the distribution network constraints after bid set activation (voltage and loading limits) for several contingency cases that should be considered to ensure (n-1) security,
- allows calculating the power of bid sets, i.e., impact of bid set activation on the active power flows through the DSO/TSO intersections.

This section presents the corresponding model that is developed within the I4RD project, which is already described in D5.1. However, this section provides all formulas necessary to understand the final process functionalities described in section 3.1. It is calculated by using local sensitivity analysis, which linearizes, for each time interval, the distribution system around a specific baseline operating point. Based on these sensitivity values, it allows estimating the baseline deviations resulting from bid set activation. Only critical elements, i.e., nodes and branches that may violate their limits after bid set activation in any contingency case, are considered by the simplified model to reduce data exchanges in the planned DSO/TSO interaction process. Sections 2.1 and 2.2 provide the mathematical description of the baseline operating point, bid sets, and baseline deviations. The equations of the simplified model are given in section 2.3.

2.1. The baseline operating point

The baseline operating point of a distribution system is defined by the loads' active and reactive power contributions according to Eq. (2.1)[1].

$$\tilde{\boldsymbol{P}}_{m,t}^{\text{base}} = \left(\tilde{P}_{m,t,1}^{\text{base}} \quad \cdots \quad \tilde{P}_{m,t,L}^{\text{base}}\right)^{\text{T}} \qquad \text{Size: } (L \times 1) \qquad (2.1a)$$

$$\tilde{\boldsymbol{Q}}_{m,t}^{\text{base}} = \left(\tilde{Q}_{m,t,1}^{\text{base}} \quad \cdots \quad \tilde{Q}_{m,t,L}^{\text{base}}\right)^{\text{T}} \qquad \text{Size: } (L \times 1) \qquad (2.1b)$$

Where m is an arbitrary contingency case; t is an arbitrary instant of time; L is the number of loads within the regarded system portion; and $\tilde{P}_{m,t,l}^{\text{base}}$, $\tilde{Q}_{m,t,l}^{\text{base}}$ are the baseline active and reactive power contributions of load l. These power contributions lead to the baseline node voltages, branch loadings, branch active power flows, and tap positions, which are given in Eq. (2.2).

$$\boldsymbol{U}_{m,t}^{\text{base}} = \left(U_{m,t,1}^{\text{base}} \quad \cdots \quad U_{m,t,N}^{\text{base}}\right)^{\text{T}} \qquad \text{Size: } (N \times 1) \qquad (2.2a)$$

$$\boldsymbol{\lambda}_{m,t}^{\text{base}} = \left(\lambda_{m,t,1}^{\text{base}} \quad \cdots \quad \lambda_{m,t,B}^{\text{base}}\right)^{\text{T}} \qquad \text{Size: } (B \times 1) \qquad (2.2b)$$

$$\boldsymbol{P}_{m,t}^{\text{base}} = \left(P_{m,t,1}^{\text{base}} \quad \cdots \quad P_{m,t,B}^{\text{base}}\right)^{\text{T}} \qquad \text{Size: } (B \times 1) \qquad (2.2c)$$

$$\boldsymbol{\theta}_{m,t}^{\text{base}} = \left(\theta_{m,t,1}^{\text{base}} \quad \cdots \quad \theta_{m,t,\rho}^{\text{base}}\right)^{\text{T}} \qquad \text{Size: } (\rho \times 1) \qquad (2.2d)$$

[1] Here the superscript "T" (non-italic) transposes the vector and should not be confused with the number of time points "T" (italic) introduced in Eq. (2.7).

Where ρ, N, B, are the numbers of on-load tap changers, critical nodes, and critical branches within the regarded system portion; $U_{m,t,n}^{\text{base}}$ is the baseline voltage magnitude of node n; $\lambda_{m,t,b}^{\text{base}}$ is the baseline loading of branch b; $P_{m,t,b}^{\text{base}}$ is the baseline active power flowing into branch b; and $\theta_{m,t,\sigma}^{\text{base}}$ is the baseline tap position of tap changer σ.

2.2. Baseline deviations

Load changes, that are induced by the activation of an arbitrary bid set, modify the baseline network state. Various loads and on-load tap changes may respond to the modified network state by adapting their power contributions and tap positions. As a result, a state of equilibrium is established, which depends on the characteristics of the loads, the tap changers, and the network.

2.2.1. The interrelations between load changes and network state

Equation (2.3) describes load changes, i.e., deviations of the loads' baseline power contributions given in Eq. (2.1).

$$\Delta\widetilde{\boldsymbol{P}}_{m,t} = \left(\Delta\tilde{P}_{m,t,1} \quad \cdots \quad \Delta\tilde{P}_{m,t,L}\right)^{\mathrm{T}} \qquad \text{Size: } (L \times 1) \qquad (2.3a)$$

$$\Delta\widetilde{\boldsymbol{Q}}_{m,t} = \left(\Delta\tilde{Q}_{m,t,1} \quad \cdots \quad \Delta\tilde{Q}_{m,t,L}\right)^{\mathrm{T}} \qquad \text{Size: } (L \times 1) \qquad (2.3b)$$

Where $\Delta\tilde{P}_{m,t,l}$, $\Delta\tilde{Q}_{m,t,l}$ describe the active and reactive power changes of load l. Such load changes modify the entire network state according to Eq. (2.4).

$$\boldsymbol{U}_{m,t}^{\text{dev}}\left(\Delta\widetilde{\boldsymbol{P}}_{m,t}, \Delta\widetilde{\boldsymbol{Q}}_{m,t}\right) = \boldsymbol{U}_{m,t}^{\text{base}} + \Delta\boldsymbol{U}_{m,t}\left(\Delta\widetilde{\boldsymbol{P}}_{m,t}, \Delta\widetilde{\boldsymbol{Q}}_{m,t}\right) \qquad \text{Size: } (N \times 1) \qquad (2.4a)$$

$$\boldsymbol{\lambda}_{m,t}^{\text{dev}}\left(\Delta\widetilde{\boldsymbol{P}}_{m,t}, \Delta\widetilde{\boldsymbol{Q}}_{m,t}\right) = \boldsymbol{\lambda}_{m,t}^{\text{base}} + \Delta\boldsymbol{\lambda}_{m,t}\left(\Delta\widetilde{\boldsymbol{P}}_{m,t}, \Delta\widetilde{\boldsymbol{Q}}_{m,t}\right) \qquad \text{Size: } (B \times 1) \qquad (2.4b)$$

$$\boldsymbol{P}_{m,t}^{\text{dev}}\left(\Delta\widetilde{\boldsymbol{P}}_{m,t}, \Delta\widetilde{\boldsymbol{Q}}_{m,t}\right) = \boldsymbol{P}_{m,t}^{\text{base}} + \Delta\boldsymbol{P}_{m,t}\left(\Delta\widetilde{\boldsymbol{P}}_{m,t}, \Delta\widetilde{\boldsymbol{Q}}_{m,t}\right) \qquad \text{Size: } (B \times 1) \qquad (2.4c)$$

Where $\boldsymbol{U}_{m,t}^{\text{dev}}$, $\boldsymbol{\lambda}_{m,t}^{\text{dev}}$, $\boldsymbol{P}_{m,t}^{\text{dev}}$ are the deviated node voltages, branch loadings, and branch active power flows; and $\Delta\boldsymbol{U}_{m,t}$, $\Delta\boldsymbol{\lambda}_{m,t}$, $\Delta\boldsymbol{P}_{m,t}$ describe the impact of load changes on the node voltages, branch loadings, and branch active power flows. As loads are generally voltage-dependent [1], they respond to the modified network state by adapting their power contributions. These voltage dependencies may be small if no distribution system controls are used and large otherwise. For instance, local controls, such as $P(U)$ and $Q(U)$ controls of photovoltaic inverters [2], may significantly adapt their active and reactive power contributions to mitigate voltage variations. This means – in the context of the planned redispatch process – that flexibility activations (⇾ direct load changes) are generally accompanied by unintended load changes of various other loads (⇾ indirect load changes). Equation (2.5) splits the load changes from Eq. (2.3) into direct ($\Delta\widetilde{\boldsymbol{P}}_{m,t}^{\text{dir}}$, $\Delta\widetilde{\boldsymbol{Q}}_{m,t}^{\text{dir}}$) and indirect load changes ($\Delta\widetilde{\boldsymbol{P}}_{m,t}^{\text{ind}}$, $\Delta\widetilde{\boldsymbol{Q}}_{m,t}^{\text{ind}}$).

$$\Delta\widetilde{\boldsymbol{P}}_{m,t} = \Delta\widetilde{\boldsymbol{P}}_{m,t}^{\text{dir}} + \Delta\widetilde{\boldsymbol{P}}_{m,t}^{\text{ind}} \qquad \text{Size: } (L \times 1) \qquad (2.5a)$$

$$\Delta\widetilde{\boldsymbol{Q}}_{m,t} = \Delta\widetilde{\boldsymbol{Q}}_{m,t}^{\text{dir}} + \Delta\widetilde{\boldsymbol{Q}}_{m,t}^{\text{ind}} \qquad \text{Size: } (L \times 1) \qquad (2.5b)$$

Furthermore, the modified network state might provoke reactions of on-load tap changers[2] according to Eq. (2.6).

$$\boldsymbol{\theta}_{m,t}^{\text{dev}}\left(\Delta\widetilde{\boldsymbol{P}}_{m,t}, \Delta\widetilde{\boldsymbol{Q}}_{m,t}\right) = \boldsymbol{\theta}_{m,t}^{\text{base}} + \Delta\boldsymbol{\theta}_{m,t}\left(\Delta\widetilde{\boldsymbol{P}}_{m,t}, \Delta\widetilde{\boldsymbol{Q}}_{m,t}\right) \qquad \text{Size: } (\rho \times 1) \qquad (2.6)$$

Where $\Delta\boldsymbol{\theta}_{m,t}$ describes the impact of the load changes on the tap positions.

[2] Other switchable equipment, such as capacitor banks, are not considered here.

2.2.2. Bids and bid sets

In general, each load may submit several redispatch bids. These bids are often associated with catch-up and anticipatory effects (see D3.3), and therefore, each bid is represented by a timeseries as in Eq. (2.7).

$$\Delta\widetilde{\boldsymbol{P}}_f^{\mathrm{bid}} = \left(\Delta\tilde{P}_{1,f}^{\mathrm{bid}} \quad \cdots \quad \Delta\tilde{P}_{T,f}^{\mathrm{bid}}\right)^{\mathrm{T}} \qquad \text{Size: } (T \times 1) \qquad (2.7a)$$

$$\Delta\widetilde{\boldsymbol{Q}}_f^{\mathrm{bid}} = \left(\Delta\tilde{Q}_{1,f}^{\mathrm{bid}} \quad \cdots \quad \Delta\tilde{Q}_{T,f}^{\mathrm{bid}}\right)^{\mathrm{T}} \qquad \text{Size: } (T \times 1) \qquad (2.7b)$$

Where T is the number of time points; and $\Delta\tilde{P}_{t,f}^{\mathrm{bid}}$, $\Delta\tilde{Q}_{t,f}^{\mathrm{bid}}$ are the active and reactive power changes at time point t offered by bid f. Usually, redispatch bids include exclusively information concerning the active power, although the bid activation may directly affect the reactive power contribution of the corresponding load (e.g., if the bidden active power change is realized by switching on or off an asynchronous machine). In this case, the direct reactive power changes associated to a certain bid may be estimated, e.g., by Eq. (2.8).

$$\Delta\widetilde{\boldsymbol{Q}}_f^{\mathrm{bid}} = \Delta\widetilde{\boldsymbol{P}}_f^{\mathrm{bid}} \cdot \tan\left(\varphi_f\right) \qquad \text{Size: } (T \times 1) \qquad (2.8)$$

Where $\cos\left(\varphi_f\right)$ is the estimated power factor associated with bid f, e.g., 0.9 inductive for industrial customers. All submitted bids are merged, for each time point, into the bid power vectors introduced by Eq. (2.9).

$$\Delta\widetilde{\boldsymbol{P}}_t^{\mathrm{bids}} = \left(\Delta\tilde{P}_{t,1}^{\mathrm{bid}} \quad \cdots \quad \Delta\tilde{P}_{t,F}^{\mathrm{bid}}\right)^{\mathrm{T}} \qquad \text{Size: } (F \times 1) \qquad (2.9a)$$

$$\Delta\widetilde{\boldsymbol{Q}}_t^{\mathrm{bids}} = \left(\Delta\tilde{Q}_{t,1}^{\mathrm{bid}} \quad \cdots \quad \Delta\tilde{Q}_{t,F}^{\mathrm{bid}}\right)^{\mathrm{T}} \qquad \text{Size: } (F \times 1) \qquad (2.9b)$$

Where F is the number of submitted bids. The timeseries of each bid are associated with one scalar cost value. The cost vector provided by Eq. (2.10) contains the costs of each submitted bid, i.e., each bid included in the bid matrices.

$$\boldsymbol{C}^{\mathrm{bids}} = \left(C_1^{\mathrm{bid}} \quad \cdots \quad C_F^{\mathrm{bid}}\right) \qquad \text{Size: } (1 \times F) \qquad (2.10)$$

Where C_f^{bid} is the cost of bid f. Each bid set has its own and unique impact on the network state. In general, bids may exclude each other (see D3.3), and therefore, the XOR-linkage matrix is introduced in Eq. (2.11).

$$\boldsymbol{\varepsilon} = \begin{pmatrix} \varepsilon_{1,1} & \cdots & \varepsilon_{1,F} \\ \vdots & \ddots & \vdots \\ \varepsilon_{F,1} & \cdots & \varepsilon_{F,F} \end{pmatrix} \qquad \text{Size: } (F \times F) \qquad (2.11)$$

Where $\varepsilon_{f_1,f_2} = 1$ if bid f_1 is XOR-linked to bid f_2 and zero otherwise. All values within the primary diagonal of this matrix are defined to be zero ($\varepsilon_{i,i} = 0, \forall i$). The decision variable $\boldsymbol{x}$ is introduced by Eq. (2.12a) to allow selecting a certain bid set from the bid matrices according to Eq. (2.12b) to (2.12d).

$$\boldsymbol{x} = \left(x_1 \quad \cdots \quad x_F\right)^{\mathrm{T}} \qquad \text{Size: } (F \times 1) \qquad (2.12a)$$

$$\Delta\widetilde{\boldsymbol{P}}_t^{\mathrm{bid\ set}}(\boldsymbol{x}) = \mathrm{diag}(\boldsymbol{x}) \cdot \Delta\widetilde{\boldsymbol{P}}_t^{\mathrm{bids}} \qquad \text{Size: } (F \times 1) \qquad (2.12b)$$

$$\Delta\widetilde{\boldsymbol{Q}}_t^{\mathrm{bid\ set}}(\boldsymbol{x}) = \mathrm{diag}(\boldsymbol{x}) \cdot \Delta\widetilde{\boldsymbol{Q}}_t^{\mathrm{bids}} \qquad \text{Size: } (F \times 1) \qquad (2.12c)$$

$$C^{\mathrm{bid\ set}}(\boldsymbol{x}) = \boldsymbol{C}^{\mathrm{bids}} \cdot \boldsymbol{x} \qquad \text{Size: } (1 \times 1) \qquad (2.12d)$$

Where x_f is one, if bid f is included in the regarded bid set, and zero otherwise; and $\Delta\widetilde{\boldsymbol{P}}_t^{\mathrm{bid\ set}}$, $\Delta\widetilde{\boldsymbol{Q}}_t^{\mathrm{bid\ set}}$ are denoted as bid set vectors. The total redispatch power ($\Delta\tilde{P}_t^{\mathrm{DSO/TSO}}$) of bid set $\boldsymbol{x}$ is calculated according to Eq. (2.13).

$$\Delta\tilde{P}_t^{\mathrm{DSO/TSO}}(\boldsymbol{x}) = \boldsymbol{x}^{\mathrm{T}} \cdot \Delta\widetilde{\boldsymbol{P}}_t^{\mathrm{bids}} \qquad \text{Size: } (1 \times 1) \qquad (2.13)$$

The number of bids does usually not match the number of loads, as not all loads submit bids, and some loads may submit multiple bids. Therefore, the bid set matrices are mapped to the direct load changes given in Eq. (2.5) according to Eq. (2.14).

$$\Delta\widetilde{\boldsymbol{P}}_t^{\mathrm{dir}}(\boldsymbol{x}) = \boldsymbol{y}\cdot\Delta\widetilde{\boldsymbol{P}}_t^{\mathrm{bid\ set}}(\boldsymbol{x}) \qquad \text{Size: } (L\times 1) \qquad (2.14a)$$

$$\Delta\widetilde{\boldsymbol{Q}}_t^{\mathrm{dir}}(\boldsymbol{x}) = \boldsymbol{y}\cdot\Delta\widetilde{\boldsymbol{Q}}_t^{\mathrm{bid\ set}}(\boldsymbol{x}) \qquad \text{Size: } (L\times 1) \qquad (2.14b)$$

$$\boldsymbol{y} = \begin{pmatrix} y_{1,1} & \cdots & y_{1,F} \\ \vdots & \ddots & \vdots \\ y_{L,1} & \cdots & y_{L,F} \end{pmatrix} \qquad \text{Size: } (L\times F) \qquad (2.14c)$$

Where $y_{l,f}$ is one, if bid f is submitted by load l, and zero otherwise; and $\boldsymbol{y}$ is denoted as bid allocation matrix.

2.3. Model equations

This section provides two sets of model equations: the complete and the reduced one. The complete set allows estimating the effect of direct and indirect load changes as well as tap reactions on the network state. Most of these inputs are unknown during process execution, and consequently, the complete set of equations is of academic interest rather than practical relevance. In contrast, the reduced set of equations neglects the unknown quantities to obtain a model than can be used in the planned DSO/TSO interaction process. However, both sets use Eq. (2.15) to calculate the node voltages and branch loadings resulting from the activation of a bid set $\boldsymbol{x}$.

$$\boldsymbol{U}_{m,t}^{\mathrm{dev,est}}(\boldsymbol{x}) = \boldsymbol{U}_{m,t}^{\mathrm{base}} + \Delta\boldsymbol{U}_{m,t}^{\mathrm{est}}(\boldsymbol{x}) \qquad \text{Size: } (N\times 1) \qquad (2.15a)$$

$$\boldsymbol{\lambda}_{m,t}^{\mathrm{dev,est}}(\boldsymbol{x}) = \boldsymbol{\lambda}_{m,t}^{\mathrm{base}} + \Delta\boldsymbol{\lambda}_{m,t}^{\mathrm{est}}(\boldsymbol{x}) \qquad \text{Size: } (B\times 1) \qquad (2.15b)$$

Where $\boldsymbol{U}_{m,t}^{\mathrm{dev,est}}$, $\boldsymbol{\lambda}_{m,t}^{\mathrm{dev,est}}$ are the estimated node voltages and branch loadings resulting from the activation of bid set $\boldsymbol{x}$; and $\Delta\boldsymbol{U}_{m,t}^{\mathrm{est}}$, $\Delta\boldsymbol{\lambda}_{m,t}^{\mathrm{est}}$ are the estimated impacts of bid set activation on the node voltages and branch loadings.

2.3.1. Complete set of equations

The activation of a bid set might provoke indirect load changes and tap reactions (see section 2.2.1). As the parameters of the simplified model cannot appropriately reflect this (generally nonlinear) behavior, the indirect load changes and tap reactions are defined as additional model inputs. Figure 2 shows the resulting inputs, outputs, and parameters of the simplified distribution system model.

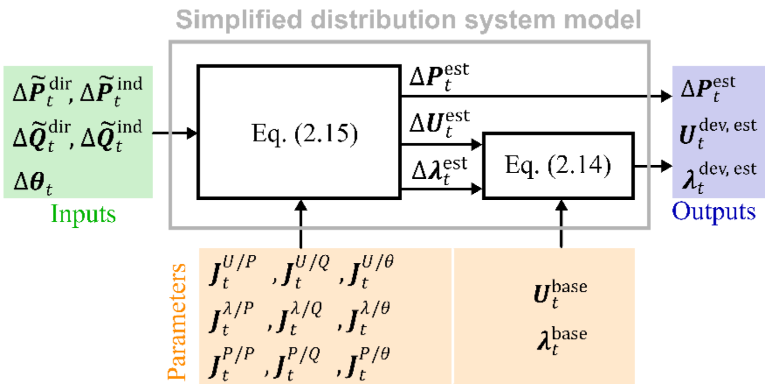

Figure 2: Inputs, outputs, and parameters of the complete simplified distribution system model.

The model uses the baseline network state and the associated sensitivity matrices to estimate the network state resulting from the activation of a certain bid set $\boldsymbol{x}$ according to Eq. (2.16).

$$\Delta\boldsymbol{U}_{m,t}^{\mathrm{est}}(\boldsymbol{x}) = \boldsymbol{J}_{m,t}^{U/P}\cdot\Delta\widetilde{\boldsymbol{P}}_{m,t}(\boldsymbol{x}) + \boldsymbol{J}_{m,t}^{U/Q}\cdot\Delta\widetilde{\boldsymbol{Q}}_{m,t}(\boldsymbol{x}) + \boldsymbol{J}_{m,t}^{U/\theta}\cdot\Delta\boldsymbol{\theta}_{m,t}(\boldsymbol{x}) \qquad \text{Size: } (N\times 1) \qquad (2.16a)$$

$$\Delta\boldsymbol{\lambda}_{m,t}^{\mathrm{est}}(\boldsymbol{x}) = \boldsymbol{J}_{m,t}^{\lambda/P}\cdot\Delta\widetilde{\boldsymbol{P}}_{m,t}(\boldsymbol{x}) + \boldsymbol{J}_{m,t}^{\lambda/Q}\cdot\Delta\widetilde{\boldsymbol{Q}}_{m,t}(\boldsymbol{x}) + \boldsymbol{J}_{m,t}^{\lambda/\theta}\cdot\Delta\boldsymbol{\theta}_{m,t}(\boldsymbol{x}) \qquad \text{Size: } (B\times 1) \qquad (2.16b)$$

$$\Delta\boldsymbol{P}_{m,t}^{\mathrm{est}}(\boldsymbol{x}) = \boldsymbol{J}_{m,t}^{P/P}\cdot\Delta\widetilde{\boldsymbol{P}}_{m,t}(\boldsymbol{x}) + \boldsymbol{J}_{m,t}^{P/Q}\cdot\Delta\widetilde{\boldsymbol{Q}}_{m,t}(\boldsymbol{x}) + \boldsymbol{J}_{m,t}^{P/\theta}\cdot\Delta\boldsymbol{\theta}_{m,t}(\boldsymbol{x}) \qquad \text{Size: } (B\times 1) \qquad (2.16c)$$

Where $\boldsymbol{J}_{m,t}^{U/P}$, $\boldsymbol{J}_{m,t}^{U/Q}$, $\boldsymbol{J}_{m,t}^{U/\theta}$ are the sensitivities of node voltages with respect to load and tap position changes; $\boldsymbol{J}_{m,t}^{\lambda/P}$, $\boldsymbol{J}_{m,t}^{\lambda/Q}$, $\boldsymbol{J}_{m,t}^{\lambda/\theta}$ are the sensitivities of branch loadings with respect to load and tap position changes; and $\boldsymbol{J}_{m,t}^{P/P}$, $\boldsymbol{J}_{m,t}^{P/Q}$, $\boldsymbol{J}_{m,t}^{P/\theta}$ are the sensitivities of branch active power flows with respect to load and tap position changes. The exact definitions of the sensitivity matrices are given in the Annex.

2.3.2. Reduced set of equations

The reduced set of equations presented in Eq. (2.17) neglects direct reactive power changes, indirect load changes and tap reactions, as these quantities are unknown during process execution. Only the direct active power changes, which correspond to the redispatch bids, are considered as model inputs. The active power flows through individual branches are not calculated; instead, only the total redispatch power is calculated according to Eq. (2.13).

$$\Delta\boldsymbol{U}_{m,t}^{\mathrm{est}}(\boldsymbol{x}) \approx \boldsymbol{J}_{m,t}^{U/P} \cdot \Delta\widetilde{\boldsymbol{P}}_{t}^{\mathrm{dir}}(\boldsymbol{x}) \quad \text{Size: } (N \times 1) \qquad (2.17a)$$

$$\Delta\boldsymbol{\lambda}_{m,t}^{\mathrm{est}}(\boldsymbol{x}) \approx \boldsymbol{J}_{m,t}^{\lambda/P} \cdot \Delta\widetilde{\boldsymbol{P}}_{t}^{\mathrm{dir}}(\boldsymbol{x}) \quad \text{Size: } (B \times 1) \qquad (2.17b)$$

However, DSOs can calculate the model parameters, i.e., the baseline network state and the sensitivity matrices, only for observable network portions. Nowadays, comprehensive observability is given only at the HV but usually not at the MV level. Consequently, as a first step, the process might be implemented only at the HV level, and the MV networks may added as soon as they are observable enough to calculate the necessary model parameters. In such a preliminary implementation, the consideration of voltage changes according to Eq. (2.17a) may be omitted as there are usually no voltage problems at the HV level.

3. The DSO/TSO interaction process

This section documents the final DSO/TSO interaction process in its entirety, accepting recurrences from D5.1 to consolidate all information relevant for process implementation into one document. Information concerning the requirements that underlie the process design can be found in D5.1. Figure 3 overviews the functionalities (orange fonts) and data exchanges (arrows) of the planned DSO/TSO interaction process (blue box). The schedules and RD bids of the flexibility providing industrial customers are inputs from WP4 and are not further elaborated in this deliverable (see section 1.2).

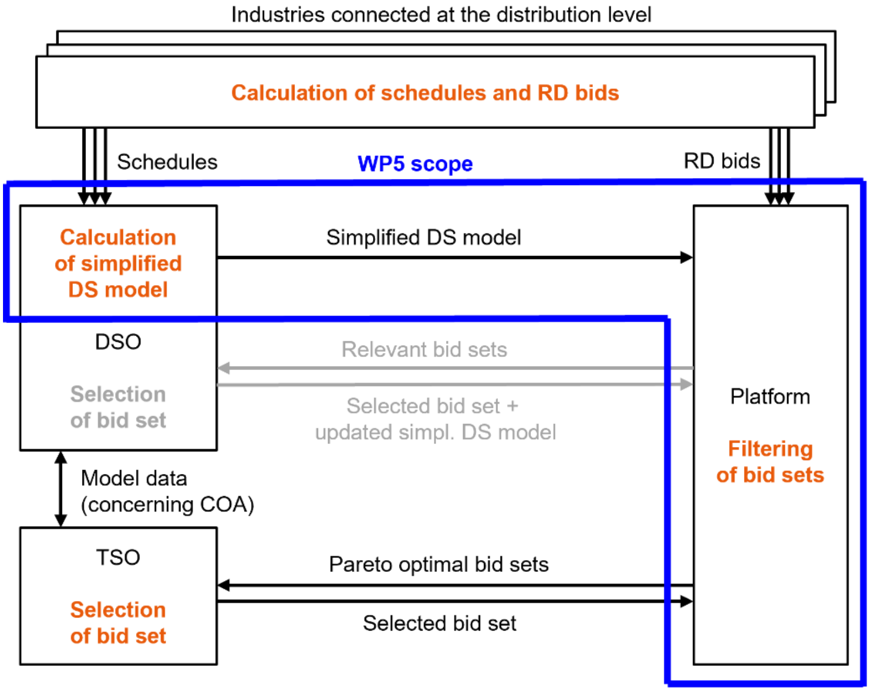

Figure 3: Functionalities and data exchanges of the planned DSO/TSO interaction process.

The major process functionalities are divided into three blocks: the *calculation of the simplified DS model*, the *filtering of bid sets*, and the *selection of a bid set*, whereby the calculation of the simplified DS model and the bid set filtering constitute the core functionalities of the planned DSO/TSO interaction process. However, before executing these functionalities, the network operators exchange relevant network model data concerning their common observability area (COA), i.e., a part of the network that is included in the models of both, the DSO and TSO. The DSO uses load flow simulations and local sensitivity analysis to calculate the parameters of the simplified model of its distribution system based on the schedules of the industrial customers and other data and sends them to the platform. The model parameters are calculated for all relevant time points and contingency cases necessary to ensure (n-1) security. The platform uses the simplified DS model to filter the bid sets for redispatch at the transmission level, i.e., it identifies the pareto optimal bid sets (optimality in costs and impact). However, if redispatch is necessary at the distribution level in any contingency case, the platform sends all relevant bids, i.e., the bids of all flexibility providing industries connected at the affected distribution network, to the corresponding DSO. In this case, the DSO selects the most suitable bid set, re-calculates its simplified DS model, and sends the relevant data back to the platform. Now, the platform uses the updated simplified DS model to filter the remaining bid sets, i.e., to calculate the pareto optimal bid sets, which do not violate any distribution network constraints (voltage and loading limits). Finally, the TSO selects the most suitable bid set for redispatch at the transmission level and reports the selection back to the platform.

3.1. Process functionalities

3.1.1. Calculation of the simplified distribution system model

The simplified DS model according to Eq. (2.15) and (2.17), which is calculated and provided by the DSO, constitutes the basis for the bid set filtering process at the platform level. Figure 4 shows the flow chart describing both the initial calculation of the simplified DS model and its re-calculation after bid set selection at the distribution level (if redispatch at the distribution level is necessary). In any case, day-ahead load flows and local sensitivities are calculated and stored in 15min time steps. The parameters of the simplified DS model are calculated for T time points and Mcontingency cases that are relevant to ensure (n-1) security, yielding $M \cdot T$ sets of model parameters in total.

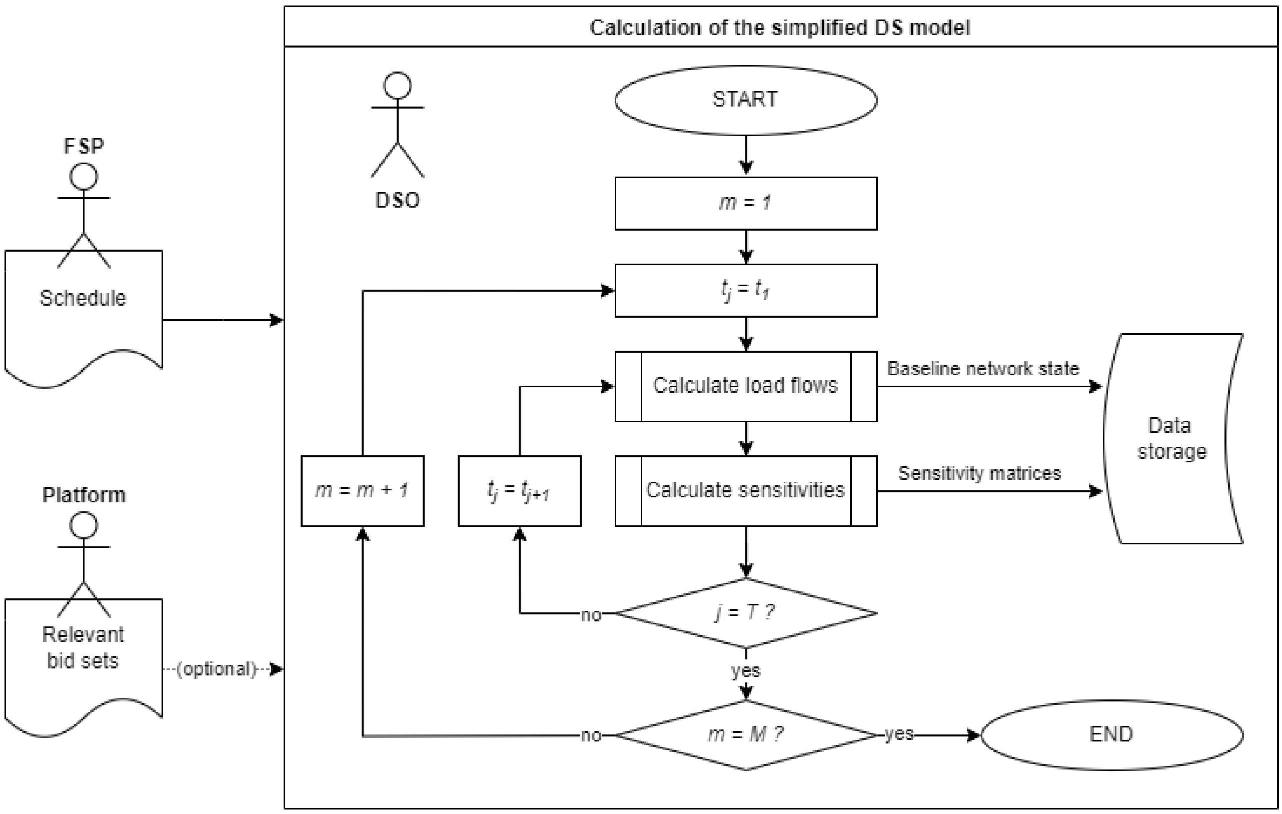

Figure 4: Flow chart describing the calculation of the simplified DS model.

The calculation of the simplified DS model requires comprehensive observability of the distribution networks, which is currently given only at the HV level.

3.1.1.1. Initial calculation

At the very beginning of the planned DSO/TSO interaction process, the DSO calculates the initial simplified DS model for the upcoming day (24h time horizon in 15min time intervals) based on the detailed DS model and the received industry schedules. Schedules of other network users and bus loads are estimated with state-of-the-art procedures, i.e., measurement- or component-based approaches [1]. No bid sets are considered in this sub-process.

3.1.1.2. Re-calculation

The DSO re-calculates the simplified DS model after receiving relevant bid sets from the platform and after selecting the most suitable bid set. This re-calculation is optional and happens only if the platform detects violations of the distribution network's operational voltage or current limits based on the initially calculated baseline network state. In contrast to the initial calculation, the re-calculation is based on the modified industry schedules, which reflect the effects of the selected bids including the corresponding anticipatory and catch-up effects (see D3.3).

3.1.2. Filtering of bid sets

The bid set filtering is the core task of the planned DSO/TSO interaction process and includes three sub-processes to counteract violations of the operational current and voltage limits at the distribution level. Figure 5 sketches the corresponding flow chart. First, the platform examines the need for redispatch at the distribution level by checking the baseline network state of all contingency cases against its operational limits. If redispatch is necessary at the distribution level in any of these cases, the platform identifies all relevant bids, i.e., bids of flexibility providing industries connected at the affected distribution network and makes them accessible to the DSO. Otherwise, it uses the simplified DS model to identify pareto optimal bid sets, i.e., sets with low cost and high power that do not provoke any limit violations at the distribution level, and makes them accessible to the TSO.

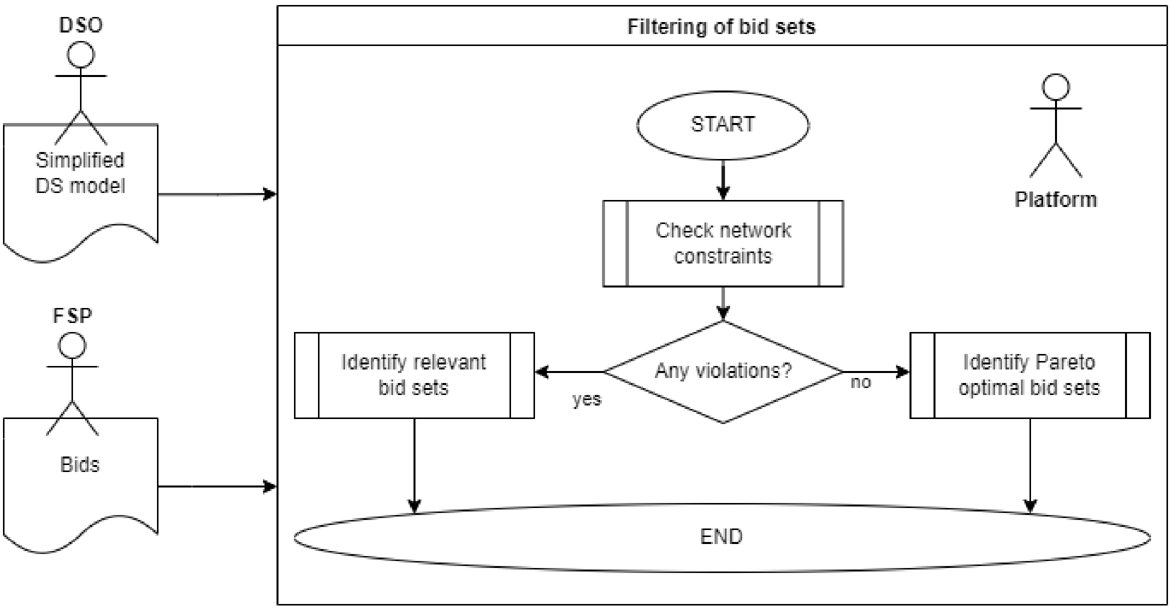

Figure 5: Flow chart describing the filtering of bid sets.

3.1.2.1. Checking the network constraints

This sub-process checks – for all contingency cases and time points – the loadings and voltages of all critical distribution branches and nodes against their limits. Limit violations are detected if any of the conditions given in Eq. (3.1) is satisfied:

$$\boldsymbol{\lambda}_{m,t}^{\text{base}} > \boldsymbol{\lambda}^{\text{max}} \qquad \forall m,t \qquad (3.1a)$$

$$\boldsymbol{U}_{m,t}^{\text{base}} > \boldsymbol{U}^{\text{max}} \qquad \forall m,t \qquad (3.1b)$$

$$\boldsymbol{U}_{m,t}^{\text{base}} < \boldsymbol{U}^{\text{min}} \qquad \forall m,t \qquad (3.1c)$$

Where $\boldsymbol{\lambda}^{\max}$, $\boldsymbol{U}^{\max}$, $\boldsymbol{U}^{\min}$ are the maximal and minimal permissible values of $\boldsymbol{\lambda}$, $\boldsymbol{U}$.

3.1.2.2. Identifying relevant bid sets for DSO

This sub-process identifies all redispatch bids of industries that are connected to the limit violating distribution network and makes them accessible to the corresponding DSO. No calculations but only geographic/topological information is necessary.

3.1.2.3. Identifying pareto optimal bid sets for TSO

Pareto optimal bid sets have low costs and high total redispatch power and can be used for redispatch at the transmission level without violating distribution network constraints. The corresponding optimization problem is formulated in Eq. (3.2), wherein the objective functions are calculated by Eq. (2.12d) and (2.13). It aims at identifying multiple feasible and reasonable bid sets by minimizing costs (for the complete time horizon, i.e., 24h) and maximizing power (for a specific time point) while respecting the distribution network constraints. The scalar constraints (3.2d-e) refuse the trivial bid set (wherein no bid is accepted) and avoid XOR conflicts between the bids. It should be noticed that the total redispatch power (second objective) is calculated for a specific time point while the constraints must be respected for all time points $t \in [1, T]$.

$$\min_{\boldsymbol{x}} f(\boldsymbol{x}) = \quad C^{\text{bid set}}(\boldsymbol{x}) \tag{3.2a}$$

$$\max_{\boldsymbol{x}} g_t(\boldsymbol{x}) = \quad \pm\Delta\tilde{P}_t^{\text{DSO/TSO}}(\boldsymbol{x}) \tag{3.2b}$$

$$\text{Subject to} \quad \begin{array}{lll}
\boldsymbol{\lambda}_{1,1}^{\text{dev,est}}(\boldsymbol{x}) - \boldsymbol{\lambda}^{\max} \leq 0 & \dots & \boldsymbol{\lambda}_{1,T}^{\text{dev,est}}(\boldsymbol{x}) - \boldsymbol{\lambda}^{\max} \leq 0 \\
\boldsymbol{U}_{1,1}^{\text{dev,est}}(\boldsymbol{x}) - \boldsymbol{U}^{\max} \leq 0 & \dots & \boldsymbol{U}_{1,T}^{\text{dev,est}}(\boldsymbol{x}) - \boldsymbol{U}^{\max} \leq 0 \\
\boldsymbol{U}^{\min} - \boldsymbol{U}_{1,1}^{\text{dev,est}}(\boldsymbol{x}) \leq 0 & \dots & \boldsymbol{U}^{\min} - \boldsymbol{U}_{1,T}^{\text{dev,est}}(\boldsymbol{x}) \leq 0 \\
\dots & \dots & \dots \\
\boldsymbol{\lambda}_{M,1}^{\text{dev,est}}(\boldsymbol{x}) - \boldsymbol{\lambda}^{\max} \leq 0 & \dots & \boldsymbol{\lambda}_{M,T}^{\text{dev,est}}(\boldsymbol{x}) - \boldsymbol{\lambda}^{\max} \leq 0 \\
\boldsymbol{U}_{M,1}^{\text{dev,est}}(\boldsymbol{x}) - \boldsymbol{U}^{\max} \leq 0 & \dots & \boldsymbol{U}_{M,T}^{\text{dev,est}}(\boldsymbol{x}) - \boldsymbol{U}^{\max} \leq 0 \\
\boldsymbol{U}^{\min} - \boldsymbol{U}_{M,1}^{\text{dev,est}}(\boldsymbol{x}) \leq 0 & \dots & \boldsymbol{U}^{\min} - \boldsymbol{U}_{M,T}^{\text{dev,est}}(\boldsymbol{x}) \leq 0
\end{array} \tag{3.2c}$$

$$1 - (1 \quad \cdots \quad 1) \cdot \boldsymbol{x} \leq 0 \tag{3.2d}$$

$$\boldsymbol{x}^{\text{T}} \cdot \boldsymbol{\varepsilon} \cdot \boldsymbol{x} = 0 \tag{3.2e}$$

Where $\boldsymbol{\lambda}_{m,t}^{\text{dev,est}}$, $\boldsymbol{U}_{m,t}^{\text{dev,est}}$ are calculated by Eq. (2.15) and (2.17), $(1 \quad \cdots \quad 1)$ is a vector of length F, and $\boldsymbol{\varepsilon}$ is introduced by Eq. (2.11). This optimization problem includes $(M \cdot T \cdot (B + 2 \cdot N) + 1)$ inequality constraints and one equality constraint and is solved in Python using the NSGA2 algorithm provided by pymoo [3], [4]. The problem is solved twice for each time point (once for each algebraic sign of $\Delta\tilde{P}_t^{\text{DSO/TSO}}$), the algorithm is parametrized as listed in the Annex, and the minimization is terminated after 10 min calculation time (for each run) to ensure timely result delivery.

3.1.3. Selection of bid set

The selection of a bid set is an optimization problem that is subject to the constraints of the distribution or transmission network.

3.1.3.1. Distribution level

The DSO receives the relevant bid sets if redispatch is necessary at the distribution level. It solves an optimal power flow problem based on its detailed system model to select the most affordable bid set that safely maintains compliance with the operational limits. This sub-process is not elaborated in detail.

3.1.3.2. Transmission level

The TSO receives pareto optimal bid sets and selects the most suitable one by solving an optimal power flow problem that respects the transmission constraints. This sub-process is not elaborated in detail.

3.2. Data exchange formats

In order to perform the demonstration of the concepts developed in D3.3, D5.1 and within this deliverable, the aforementioned data must be transmitted between the participating project partners and the data exchanges must be facilitated within a suitable IT infrastructure. For the demonstration the data exchanges as depicted in Figure **3** are translated to the implementation depicted in Figure 6. The main exchanges for this process are the DS capacities, i.e., the simplified DS model, exchanged with the demonstration facility (section 3.2.1), the redispatch bids provided by the flexibility service providers (section 3.2.2), and the communication of the pareto optimal bid sets to the TSO (section 3.2.3).

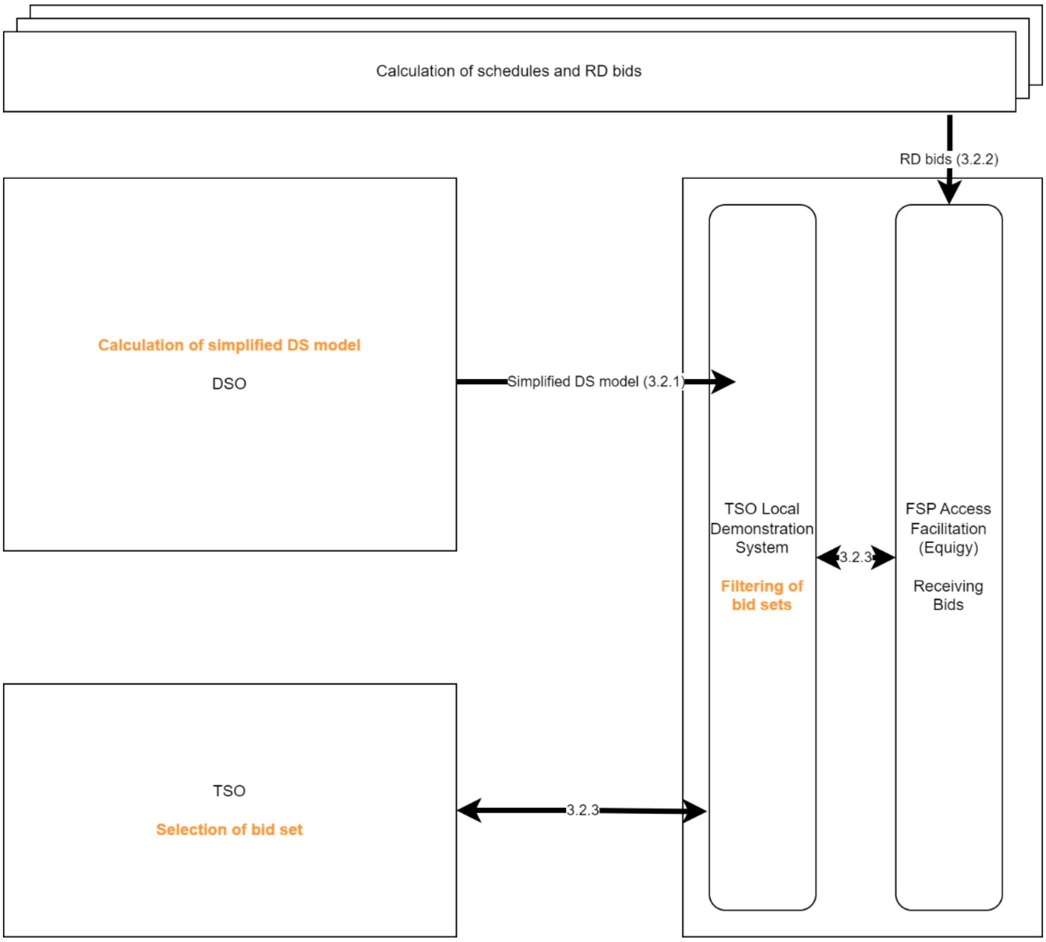

Figure 6: Implemented data exchanges.

3.2.1. DSO to platform

For calculating the pareto optimal bid sets, the platform needs the simplified DS model according to Eq. (2.15) and (2.17) as well as the respective limits of network elements. In addition to the mathematical problem statement for the application of system security limits, the TSO-DSO interaction requires further data exchanges. This data serves to integrate the mathematical optimization in the full business process. The following considerations were made by the project team and should be considered in the TSO-DSO data exchange.

3.2.1.1. General considerations

1:n relationship between platform and system operators providing data: The platform receiving the capacity information is not only interacting with one, but with many DSOs. This requires that capacity data can be traced to its source, to ensure proper mapping between flexibility bids, the master data of FSPs and the location with respect to DSO capacity data. This also ensures proper tracing of errors in case of missing capacity data.

Metadata: In addition to the origin of capacity information, further metadata must be provided. Capacity data should contain a version identification, if data must be retransmitted or updated for reasons such as process errors, faulty input data or manual process changes. In addition to a version identification, a creation timestamp is advised as to allow tracing of process delays. The data should also contain a label, indicating which process the data was intended for. In a future system of TSO-DSO coordination, redispatch planning will take place on a day-ahead, intraday, and real-time level. For each of these processes, capacity data might be exchanged so the data must be clearly associated with the intended process.

Time resolution – hourly but suitable for expansion: Capacity data must be transmitted for an entire business day. Depending on the resolution of congestion forecasting processes, capacity data can be calculated at different time resolutions. At the moment an hourly resolution is foreseen and a change towards 15-minute intervals needs to be anticipated for the future. A data format for capacity exchange should consider that the interaction process may benefit from a transmission of bundled timeseries, describing the entire business day or a selected period thereof, instead of individual files.

Critical elements and nodes of influence: The Jacobian matrices $\boldsymbol{J}_{m,t}^{U/P}$, $\boldsymbol{J}_{m,t}^{\lambda/P}$ must be transmitted only for critical elements (i.e., elements that the DSO wants to protect against loading and voltage limit violations) and for the nodes of influence (i.e., nodes where participating industries are connected), but not for all branches/nodes and loads. The size of these matrices may vary over time as the distribution grid may be extended or reinforced and the number of participating industries may increase. Thus, the data format must consider the varying matrix sizes and maintain the correct association between the critical elements and the nodes of influence by labeling each row and column according to the affected constraint name and the influencing nodes.

Contingency States: Grid security and capacity calculations are not only required for the expected n-state network topology but all TSOs and DSOs that adhere to the n-1 criterium in their gird, or in a part of their grid, must also calculate any security constraints of network elements for certain contingency cases. This may for example be the tripping of a line or transformer. This means that the simplified DS model must be calculated and transmitted for the n-state and all relevant contingencies. To ensure transparency in the application of constraints the resulting n-1 or n-m constraints should be labeled regarding the outage the constraint is associated with.

Types of constraints: The data format must cover loading and voltage constraints. Additionally, the format should be able to represent general linear constraints by a DSO to account for any constraints that cannot be directly attributed to a loading or voltage constraint but that might yet be necessary to ensure secure grid operations. Such limits can be required due to stability or other system constraints.

Existing formats and data exchanges: While not a necessary requirement, the consideration of other formats for TSO and DSO data exchange can provide a template for a new capacity data exchange. ENTSO-E provides data formats for an xml-based data exchange through their Electronic Data Interchange (EDI) Library [5] showing examples of how capacity data could be exchanged. Also, a data format for the exchange of the flow-based information exists for the current Core CCR capacity calculation process.

3.2.1.2. Data exchange format design

Considering the above-discussed aspects, the capacity data exchange is designed as an xml-Format suitable to transmit the required information. A tabular overview of its contents is provided in Table 1. The naming is based on the current core-convention.

Table 1: Metadata for TSO-DSO interaction.

Data	Example
Document Type	Grid Capacities
Document version	1

Process Type	AXX [3]– TSO-DSO Capacity Management
Sender identification	DSO A
Sender Role	Capacity Provider
Receiver Identification	Redispatch Platform
Receiver Role	Capacity Manager
Creation Datetime	DD.MM.YYYY HH:MM:SS
Capacity Daterange	DD.MM.YYYY HH:MM:SS - DD.MM.YYYY HH:MM:SS
Capacity Timeseries	One or more timeseries elements, each consisting of: • Position/Time Unit • List of loading constraints and nodal influencing factors • List of voltage constraints and nodal influencing factors • List of other constraints and nodal influencing factors

3.2.2. FSP to platform

The data exchange between the platform and FSP is facilitated via a Representational State Transfer (REST) API using oauth2 and transmitting data in JSON format. FSPs register with the TSO. This registration is performed via e-Mail to the TSO. After the initial registration FSPs are provided with their API endpoints and the authentication keys. A registered FSP may interact with the platform via five different information exchanges which describe the different data laid out in D3.3:

- Resource group (pool) registration.
- Asset/Resource registration.
- Resource-Group Relation.
- Flexibility Offer[4] and Offer Acknowledgement.
- Bid accept (flex offer award) message and acknowledgement.

The resource registration is used to provide additional master data related to the specific flexible device. Resource groups are formed by combining different devices. The groups are registered via the group registration form. After a resource group has been established resources can be linked to their groups via the resource-group relation data exchange. The respective JSON formats and a respective implementation guide will be shared with the FSPs operators as part of the WP 9. Bids should be transmitted as either 15-minute or hourly bids as to be compatible with the simplification regarding time-coupling described in the following section.

3.2.3. Platform to TSO

The infrastructure for the demonstration in WP9 is hosted at the TSO facilities. Thus, a formal specification for the communication between the platform and the TSO is not required within this project. Instead, a graphical user interface will be provided to the TSOs operational planning. The platform implements the process described in Figure 3, generating grid compatible and pareto-optimal combinations of flexibility bids from the bid provided by the FSPs.

These bid-sets should be generated for every distribution grid area that is subject to the TSO-DSO. The interaction process is then required to package the bid sets in a data-exchange format which should contain information about

- the distribution grid area associated with the list of bid-sets

[3] An official process type for this data exchange is not yet available

[4] And Resource Document

- the respective price-volume curve of bids-sets ranging from the maximum power reduction up to the maximum infeed
- the list of bids associated with each point in the price-volume curve

This information can then be passed on to either a human operator, an international process making of flexibility in Austria, or a national DSO. While a future implementation will need to include a data format to exchange this data the implementation for the demonstration focuses on the visualization for TSO use. The solution of the interaction process is simplified by performing only 15-minute and hourly calculations without time-coupling thus generating only 15-minute or hourly price-volume curves for each market-time unit and area of a distribution network. These price-volume curves shall be visualized as part of WP 9.

Redispatch at the transmission level requires a visualization that provides a comparative geographic overview of available redispatch capacities, giving the operational planner an immediate picture where the most optimal capacities are available. The graphical user-interface should also allow the selection of bid-sets from the price-volume curves and the and automatic selection of the associated bids. After selecting the bids, the activation by the operator then triggers the communication to the requested FSPs.

3.2.4. Other data exchanges

Besides the consideration of grid capacity constraints, the TSO-DSO interaction also requires other data exchanges that are outside the scope of the project but should be listed nonetheless.

- Schedules: Schedules of power generation and load are the basis for grid security analysis and capacity calculation. Any schedules required to perform the capacity calculation are exchanged within the existing framework for the exchange of schedules pursuant to Austrian SoMa.
- Measurement Data: Measurement data for ex-post validation will not yet be harmonized but exchanged manually after the demonstration was completed.
- Bid sets between Platform and TSO/DSO: As outlined in section 3.2.3, the framework for the demonstration does not yet require a data-exchange of bid-sets between the platform and the TSO. If the platform is to be used for the further use-cases, as depicted in UC5 and UC6a[5], a data-format for the exchange of bids and bid-sets between different users of the platform is required.

4. Simulation environment and studies

This section overviews the simulation environment, which is developed to enable the analysis of the simplified DS model, to pre-validate the DSO/TSO interaction process, and to conduct the scalability analysis in WP8 of this project. Furthermore, it presents the most relevant simulation results to provide deep insights into the suitability of the simplified DS model, the derived optimization problem formulation, and the NSGA2 algorithm.

4.1. Description of the simulation environment

Figure 7 shows that the developed environment is set up in DIgSILENT Power Factory [6] and Python [7], which communicate through an application programming interface (API), and contains several functionalities that facilitate three major tasks: 1) scenario definition, 2) process simulation, and 3) process evaluation.

As the number of bid sets rapidly increases with an increasing bid number (N bids → 2^N bid sets, if no XOR links exist), particular attention is paid to developing efficient code with low computing times and memory requirements, especially for process and model evaluation. The biggest levers to increase this efficiency are the use of parallel

[5] See Deliverable D3.1

computations, minimizing communication via the API, and avoiding the computation and storage of identical network states (different bid sets may be identical at a specific time point).

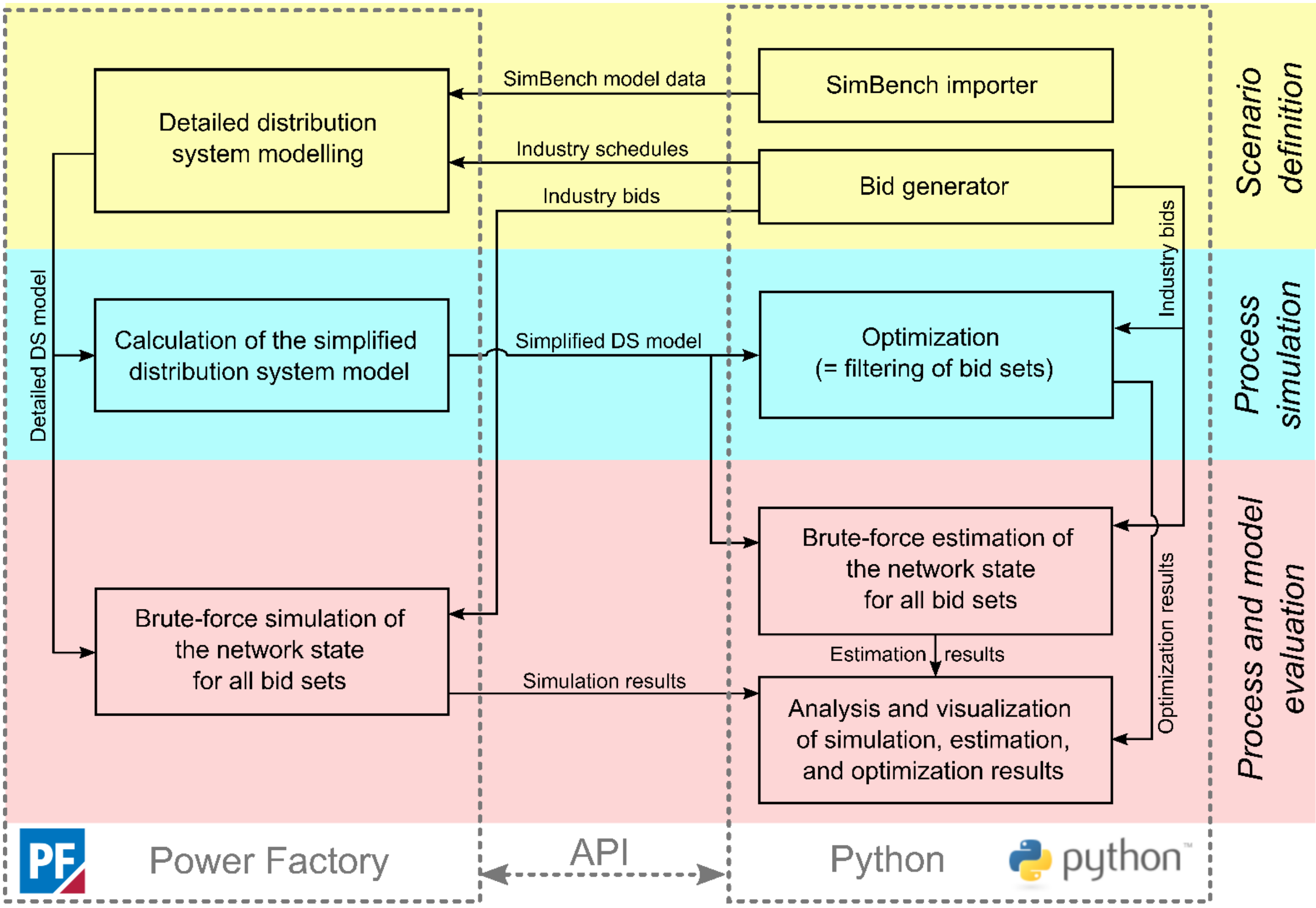

Figure 7: Overview of the developed simulation environment.

4.1.1. Scenario definition

The SimBench dataset [8] constitutes the basis of all scenarios analyzed in this deliverable. The dedicated importer automatically imports selected SimBench models to Power Factory and modifies some settings (e.g., activate on-load tap changers and $Q(U)$-controls of photovoltaic and wind turbine systems).

Based on the knowledge base of the industrial flexibility potential analysis (see D3.4) a flexibility **bid generator** was set up in Python, to generate flexibility bids for the scenario calculations.

Compared to the evaluated flexible processes in D3.4 the following subset of industrial flexibility sources for a generic area was predefined for the flexibility gid generator:

- wood grinders for mechanical pulp production in the pulp and paper sector
- power-to-heat boilers
- grinders in concrete mills
- electric drives of refrigeration units
- back-pressure steam turbines and
- gas turbines

For those flexibility sources characteristics and features for providing flexibility have been defined. Those features are provided in a data table and are described in the following. An example how this table could look like is shown in Table **2**.

First, the process type was set. This feature is later used to consider differences for the bid generation. It was distinguished between processes from the energy-intensive industry, processes from the energy-extensive sectors, auto production (of electricity) and power-to-heat assets. The first are directly related to the production process and have, thus, a limited frequency of flexibility provision. It was defined on which voltage level the site and thus the process operates. Here, high voltage and medium voltage are possible choices. Furthermore, it was characterized whether the source is a generation (e.g., turbines) or a load (processes or power-to-heat) asset, and it was defined whether a flexibility bid of that process leads to catch-up or anticipatory effects and whether a provided bid is exclusive or not. For exclusive bids "XOR bids" were built in the bid generator. Furthermore, two quantitative parameters were defined. The duration of a flexibility bid in hours – here values between one and six hours were defined as well as the call frequency per day considering how many bids are possible per day.

Table 2: Example of asset characterization.

ID	name	voltage_ level	process_ type	asset_ type	flex_ type	installed_ capacity	flex_ capacity	flex_ duration	is_ catchup	num_exclusive_ variants	call_freq _day
1	Holzschleifer_1	high_voltage	intensive	load	positive	35	7	6	False	3	1
2	P2H_1	high_voltage	P2H	load	negative	29	10	3	False	0	8
..	…	…	…	…	…	…	…	…	…	…	…
4	Muehle_2	medium_voltage	intensive	load	positive	9	9	6	False	3	1

Those process parameters are used by the bid generator, where the following (further) input parameters need to be specified in the python code:

- **Derive_exclusive_bids:** this setting can be either "True" or "False". For processes with the "num_exclusive_variants" setting is > 0 XOR-bids are derived.
- **temporal_resolution = '1h'** or **'15min'** – temporal resolution for bid generation
- **bid_number_threshold = [int, None] –** Limitation of the number of bids. For this purpose, all bids are created and randomized bids (including their exclusive bid variants) are selected.
- **Hull_curve** = 4 (default) – Envelope, duration until catch-up effect can start after bid end

The following parameters are specified and used to determine bid costs.

- *Electricity_price* in €/MWh
- *Natural_gas_price* in €/MWh
- *Emission_certificate_price* in €/t_{CO2}
- *Emission_factor* in t_{CO2}/MWh
- *Flex_effort_price* in €/MWh
- *GT_efficiency* – Conversion efficiency of gas turbines in %
- *BPT_efficiency* – Conversion efficiency of back-pressure turbines in %

The generated bids are exported in JSON format and as Excel spreadsheet. The exported JSON-file includes all bids and the following information:

- bid_id: 5-digit ID
- bid_energy: Flexible energy in MWh
- bid_size: Flexible power in MW
- bid_costs: Bid cost in €
- asset_name: Name of the flexible asset
- Sector: Choice from the set [Food, Iron_steel, Chemical, Paper]
- location: name of the location
- Voltage level: [Medium_voltage, High_voltage]
- bid_start_time: Start time of the bid '%H:%M'.
- bid_end_time: End time of the bid '%H:%M'.
- flex duration: Duration of the bid in h
- asset type: Choice from the set [load, generation]
- flex type: Choice from the set [positive, negative]
- process_type: Choice from the set [intensive, extensive, autogeneration, P2H]
- is_catchup: bid is subject to catchup effects [True, False]

- is_exclusive: bid call excludes calling of other bids. [True, False]
- excluded_bid_ids: IDs of bids excluded by call of the respective bid.
- Baseline_profiles: Baseline profiles in MW in 15min or 1h values.
- Bid_profiles: Bid profile relative to baseline in MW in 15min or 1h values.
- Catchup_profiles: Catch-up effects relative to baseline in MW in 15min- resp. 1h-values

The resulting detailed DS model and industry bids are available for process simulation and evaluation.

4.1.2. Process simulation

Power Factory calculates the parameters of the simplified DS model (baseline network state and sensitivity matrices) based on the detailed one as described in section 3.1.1.1 and provides it to the Python module, which filters all combinations of industry bids by using the NSGA2 algorithm provided by pymoo [3] to solve the optimization problem formulated in section 3.1.2.3.

4.1.3. Process and model evaluation

Several functionalities are developed to enable the comprehensive process and model evaluation, i.e., the simulation and estimation of the network state for all bid sets and the analysis and visualization of simulation, estimation, and optimization results.

4.1.3.1. Brute-force simulation of the network state for all bid sets

This module conducts load flow simulations based on the detailed DS model to calculate the optimization objectives and constraints for all relevant bid sets. The obtained results are regarded as a reference to evaluate the suitability of the optimization problem formulation.

4.1.3.2. Brute-force estimation of the network state for all bid sets

This module uses the simplified DS model to calculate the optimization objectives and constraints for all relevant bid sets. The results generated by this module provide a reference to evaluate the suitability of the NSGA2 algorithm to solve the formulated optimization problem.

4.1.3.3. Analysis and visualization of simulation, estimation, and optimization results

The simulation, estimation, and optimization modules provide tremendous amounts of data that must be analyzed and visualized to draw meaningful conclusions. They are used to generate several plots (see Figure **9** to Figure **15**) and to calculate the absolute estimation errors according to Eq. (4.1) and (4.2). Here, the subscript m is omitted in all formulas as only one case (no contingency, i.e., all lines and transformers in service) is analyzed within chapter 4; (n-1) security is considered by setting the loading limit of HV equipment to 50 %. The actual impact of bid set $\boldsymbol{x}$ on the node voltages, branch loadings, and active power flows is calculated according to Eq. (4.1), wherein $\boldsymbol{U}_t^{\text{dev,act}}$, $\boldsymbol{\lambda}_t^{\text{dev,act}}$, $\boldsymbol{P}_t^{\text{dev,act}}$ are obtained from the simulation results and $\boldsymbol{U}_t^{\text{base}}$, $\boldsymbol{\lambda}_t^{\text{base}}$, $\boldsymbol{P}_t^{\text{base}}$ from the parameters of the simplified DS model.

$$\Delta\boldsymbol{U}_t^{\text{act}}(\boldsymbol{x}) = \boldsymbol{U}_t^{\text{dev,act}}(\boldsymbol{x}) - \boldsymbol{U}_t^{\text{base}} \qquad \text{Size: } (N \times 1) \qquad (4.1a)$$

$$\Delta\boldsymbol{\lambda}_t^{\text{act}}(\boldsymbol{x}) = \boldsymbol{\lambda}_t^{\text{dev,act}}(\boldsymbol{x}) - \boldsymbol{\lambda}_t^{\text{base}} \qquad \text{Size: } (B \times 1) \qquad (4.1b)$$

$$\Delta\boldsymbol{P}_t^{\text{act}}(\boldsymbol{x}) = \boldsymbol{P}_t^{\text{dev,act}}(\boldsymbol{x}) - \boldsymbol{P}_t^{\text{base}} \qquad \text{Size: } (B \times 1) \qquad (4.1c)$$

The absolute estimation errors of each relevant bid set are calculated by Eq. (4.2) based on the estimation results ($\Delta\boldsymbol{U}_t^{\text{est}}$, $\Delta\boldsymbol{\lambda}_t^{\text{est}}$, $\Delta\boldsymbol{P}_t^{\text{est}}$) and the results of Eq. (4.1)

$$\Delta\boldsymbol{U}_t^{\text{err}}(\boldsymbol{x}) = \Delta\boldsymbol{U}_t^{\text{est}}(\boldsymbol{x}) - \Delta\boldsymbol{U}_t^{\text{act}}(\boldsymbol{x}) \qquad \text{Size: } (N \times 1) \qquad (4.2a)$$

$$\Delta\boldsymbol{\lambda}_t^{\text{err}}(\boldsymbol{x}) = \Delta\boldsymbol{\lambda}_t^{\text{est}}(\boldsymbol{x}) - \Delta\boldsymbol{\lambda}_t^{\text{act}}(\boldsymbol{x}) \qquad \text{Size: } (B \times 1) \qquad (4.2b)$$

$$\Delta\boldsymbol{P}_t^{\text{err}}(\boldsymbol{x}) = \Delta\boldsymbol{P}_t^{\text{est}}(\boldsymbol{x}) - \Delta\boldsymbol{P}_t^{\text{act}}(\boldsymbol{x}) \qquad \text{Size: } (B \times 1) \qquad (4.2c)$$

4.2. Analysis of the simplified DS model

The developed simulation environment is used to analyze the accuracy of the simplified DS model, which is given in Eq. (2.15) and (2.16), concerning voltage, loading, and active power estimations. This analysis, which is also published in [9], allows evaluating the suitability of the formulated optimization problem (as the constraints are calculated based on the simplified DS model).

4.2.1. Test system description

The analysis of the simplified DS model requires a detailed distribution system model that contains a baseline scenario and test cases that cause baseline deviations.

4.2.1.1. Baseline scenario

The baseline scenario specifies the detailed distribution system model, which includes the network and all connected elements. The correct modelling of voltage dependencies is crucial to analyze the effect of indirect load changes and tap reactions on the accuracy of the simplified DS model. Figure 8 shows the SimBench [9] distribution system model[6], which constitutes the foundation of the specified baseline scenario. One HV (110 kV) and one MV (20 kV) network are modelled in detail, and the neighboring grid parts are represented by lumped models. Local $Q(U)$ controls are added to the photovoltaic and wind turbine systems, and the HV/MV transformers have locally controlled on-load tap changers. All OLTCs keep their secondary voltages between 0.99 and 1.01 p.u. (default setting) and the used $Q(U)$ control characteristics are given in Table 8 and Figure 16 in the Annex. The 20 kV network is operated radial as the relevant switches are opened. The 110 kV grid is regarded to be operated by the DSO and has three DSO/TSO intersections, i.e., one to the 220 kV level and two to the 380 kV level.

[6] sb-code: “1-HVMV-mixed-1.105-2-no_sw”; scenario: “lPV”.

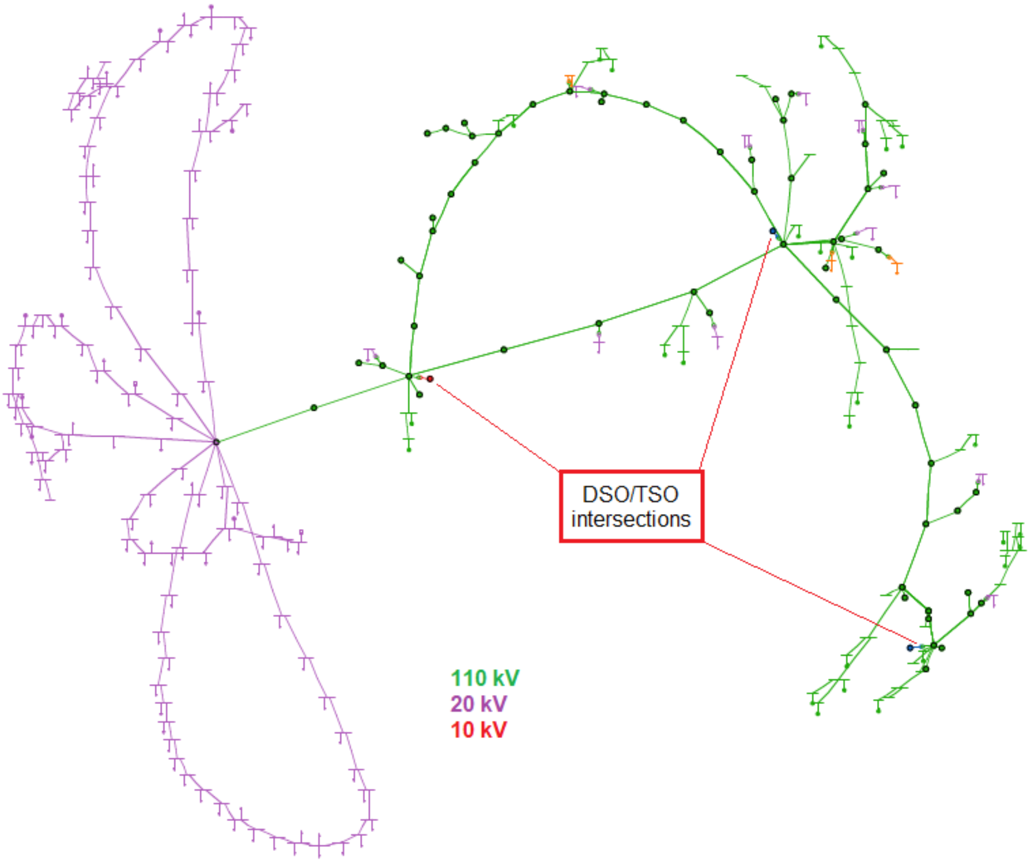

Figure 8: Distribution system model used for the simulation studies presented in this deliverable.

The chain modeling procedure described in [10] is used to model the neighboring network parts, which are represented by lumped models. The following calculations are conducted prior to the actual analyses to parametrize the lumped models of the neighboring grid parts:

1. The low voltage networks are modeled in detail, and the photovoltaic systems are equipped with $Q(U)$ control. The slack node-element is set to the primary busbar of the distribution transformer. The slack voltage is varied between 0.9 and 1.1 p.u. in small steps and the resulting $Q(U)$ and $P(U)$ characteristics at the slack node-element are recorded. These characteristics accurately reflect the aggregate behavior of the corresponding low voltage network.
2. The medium voltage grids are modeled in detail, and the photovoltaic and wind turbine systems are equipped with Q(U) control. The slack is set to the secondary busbar of the supplying transformer. The connected low voltage grids are represented by lumped models that include the previously recorded $Q(U)$ and $P(U)$ characteristics. The slack voltage is varied between 0.9 and 1.1 p.u. and the resulting $Q(U)$ and $P(U)$ characteristics at the slack element are recorded. These characteristics accurately reflect the aggregate behavior of the corresponding medium voltage network.

All lumped models shown in Figure 8 include recorded $Q(U)$ and $P(U)$ characteristics that reflect the actual behavior of the neighboring network parts. Consequently, the model yields the same results (if the slack voltage is varied in sufficient resolution) as a model that includes detailed representations of all medium and low voltage networks (which would be too large to calculate). This approach is necessary to accurately model the behavior of $Q(U)$ controls located within neighboring network parts that are represented by lumped models [11].

No contingency cases are considered for the analysis of the simplified model but only the case without any contingencies (all lines and transformers are in service).

4.2.1.2. Test cases

The test cases used to analyze the accuracy of the simplified DS model are overviewed in Table 3. The first test case corresponds to an additional absorption at the MV level: 15 loads are connected at various nodes of the 20 kV network, each consuming 1 MW during the complete 24h time horizon. Similar test cases are defined for additional injections at the MV level, as well as for additional consumptions and injections at the HV level. A power factor of 0.9 inductive is used to consider the impact of direct reactive power changes on the estimation accuracy.

Table 3: Test case for the analysis of the simplified DS model.

Test case	Level	Number of loads	Active power consumption per load	Power factor
1	MV	15	1 MW	0.9 ind.
2	MV	15	-1 MW	0.9 ind.
3	HV	10	15 MW	0.9 ind.
4	HV	10	-15 MW	0.9 ind.

4.2.2. Evaluation methodology

The parameters of the simplified model are calculated in Power Factory based on the detailed distribution model described in section 4.2.1.1. Furthermore, load flow simulations are conducted to determine the network states resulting from the test cases specified in Table 3. All nodes and branches whose baseline ($U_{t,n}^{\mathrm{base}}$, $\lambda_{t,b}^{\mathrm{base}}$) and simulated values ($U_{t,n}^{\mathrm{dev,act}}$, $\lambda_{t,n}^{\mathrm{dev,act}}$) violate the voltage and loading limits given in Table 4 are regarded as critical elements; only these elements are considered for the evaluation of the simplified DS model.

Table 4: Voltage and current limits used to classify elements as critical.

Level	Lower voltage limit	Upper voltage limit	Loading limit
HV	0.92 p.u.	1.03 p.u.	40 %
MV	0.97 p.u.	1.03 p.u.	80 %

The estimations are conducted by considering different model inputs:

1. $\Delta\widetilde{\boldsymbol{P}}_t^{\mathrm{dir}}$,
2. $\Delta\widetilde{\boldsymbol{P}}_t^{\mathrm{dir}}$ and $\Delta\widetilde{\boldsymbol{Q}}_t^{\mathrm{dir}}$,
3. $\Delta\widetilde{\boldsymbol{P}}_t^{\mathrm{dir}}$, $\Delta\widetilde{\boldsymbol{Q}}_t^{\mathrm{dir}}$, and $\Delta\boldsymbol{\theta}_t$, and
4. $\Delta\widetilde{\boldsymbol{P}}_t^{\mathrm{dir}}$, $\Delta\widetilde{\boldsymbol{Q}}_t^{\mathrm{dir}}$, $\Delta\widetilde{\boldsymbol{P}}_t^{\mathrm{ind}}$, $\Delta\widetilde{\boldsymbol{Q}}_t^{\mathrm{ind}}$, and $\Delta\boldsymbol{\theta}_t$.

Neglected inputs are set to zero. Although the true values of $\Delta\widetilde{\boldsymbol{Q}}_t^{\mathrm{dir}}$, $\Delta\widetilde{\boldsymbol{P}}_t^{\mathrm{ind}}$, $\Delta\widetilde{\boldsymbol{Q}}_t^{\mathrm{ind}}$, and $\Delta\boldsymbol{\theta}_t$ are unknown during process execution, they can be obtained from the load flow results in the described study. The absolute estimation errors are calculated for the critical elements; results are visualized and analyzed in section 4.2.3.

4.2.3. Evaluation results

We investigate the absolute voltage, loading, and active power estimation errors [Eq. (4.2)] versus the actual effects of the baseline deviations [Eq. (4.1)] for each time interval. The estimations of the branch loadings and active power flows perform significantly better than the voltage estimation [Figure **9**, Figure **10**]. The relative errors are less than 10% for most loading and active power flow estimates, while much larger errors occur for the voltage estimates:

First, we consider only additional absorptions at the MV level [Figure **9**a]. Considering only direct active power changes yields absolute estimation error magnitudes below 0.014 p.u., whereby around 95.9 % of all estimates have relative errors above 10 %. Higher error magnitudes up to 0.027 p.u. are obtained when both direct active and reactive power changes are considered. In this case, around 93.2 % of all values have a relative error above 10 %. When all inputs are considered, only 99.1 % of all estimates have relative errors above 10 %, and the maximal absolute error amounts to 0.011 p.u. Here, the indirect load changes have a low impact on the estimation accuracy in this case.

Second, we consider additional injections at the MV level [Figure **9**b]. If all inputs are known, 42.1 % of the voltage estimations yield relative errors above 10 %; the absolute errors lie between -0.003 and 0.006 p.u. In this case, the neglection of indirect load changes significantly worsens estimation accuracy: The absolute errors reach up to 0.018 p.u., and all relative errors exceed 10 %. Considering only direct load changes increases the maximal absolute error magnitude up to 0.033 p.u., and 19 % of all estimates have relative errors above 100 %. When only direct active power changes are considered, the absolute errors lie between -0.008 and 0.003 p.u., and 71.2% of all plotted values have a relative error above 10%.

Third, we consider additional absorptions at the HV level [Figure 10a]. The voltage estimation yields absolute errors up to 0.017 p.u. Most relative errors are between 10 and 100 %, even if all model inputs are considered. Neglecting tap reactions does not significantly impact the estimation accuracy.

Finally, we consider additional injections at the HV level [Figure 10b]. If all model inputs are considered, the absolute estimation error magnitudes reach up to 0.003 p.u. and around 77.8 % of all plotted values have relative errors above 10 %. Neglecting indirect load changes yields absolute errors up to 0.011 p.u.; 75.4 and 3.4 % of the estimates have relative errors above 10 % and 100 %, respectively. Again, the neglection of tap changers has no significant impact on the estimation accuracy. If only direct load changes are considered, absolute errors of -0.008 p.u. occur. All relative errors exceed 10 % and 24.4 % of all relative errors lie beyond 100 %.

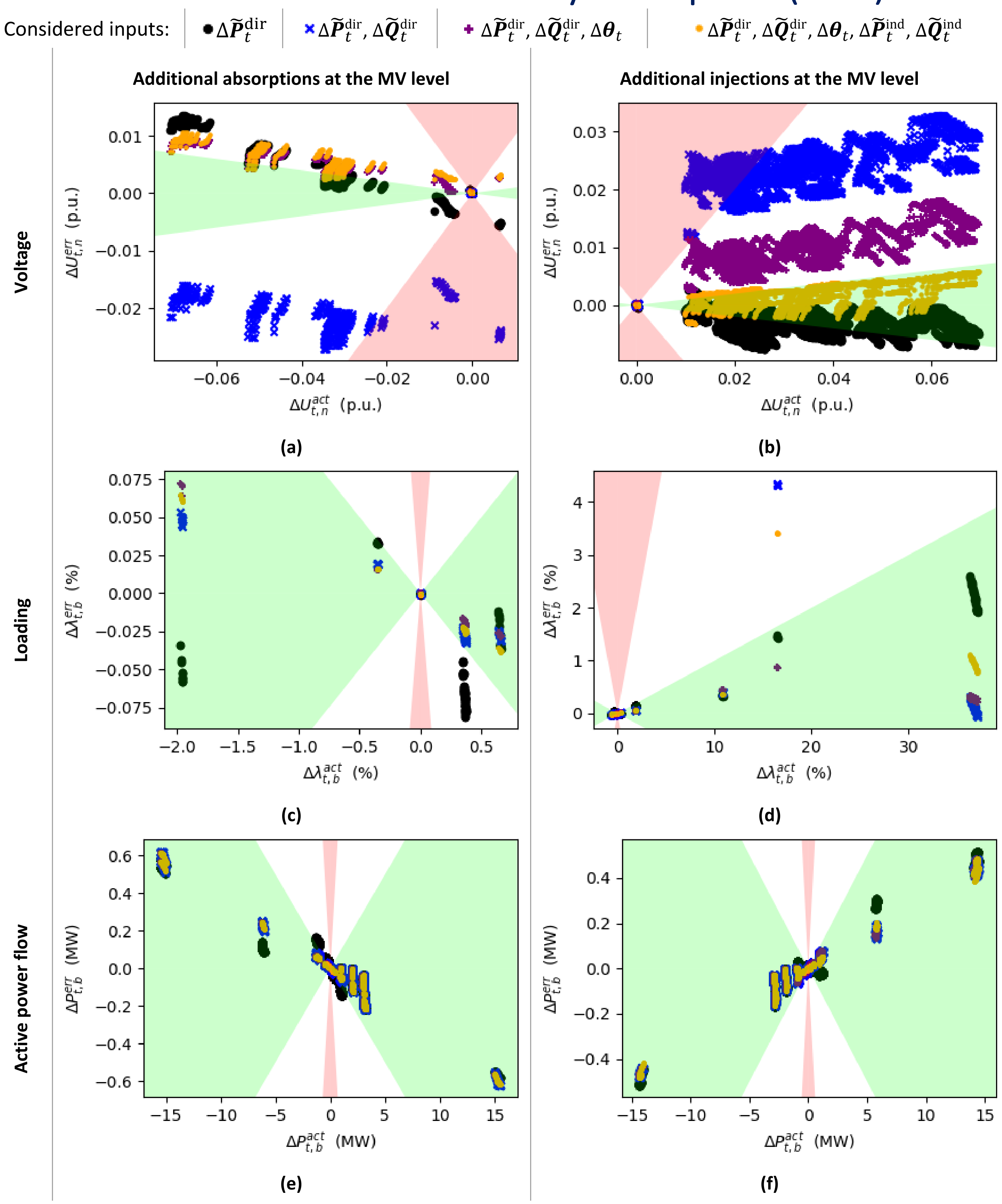

Figure 9: Absolute estimation errors for all relevant elements, time intervals, and additional absorptions / injections at the MV level: (a) voltage errors for absorptions; (b) voltage errors for injections; (c) loading errors for absorptions; (d) loading errors for injections; (e) active power errors for absorptions; (f) active power errors for injections. Voltage and loading errors are plotted only for the critical elements, and the active power flows are plotted for all branches. Areas with relative errors above 100 % and below 10 % are marked by red and green backgrounds, respectively. Different markers show which model inputs are considered: black dot → direct active power changes; blue x → direct power changes; purple plus → tap position and direct power changes; yellow dot → all inputs.

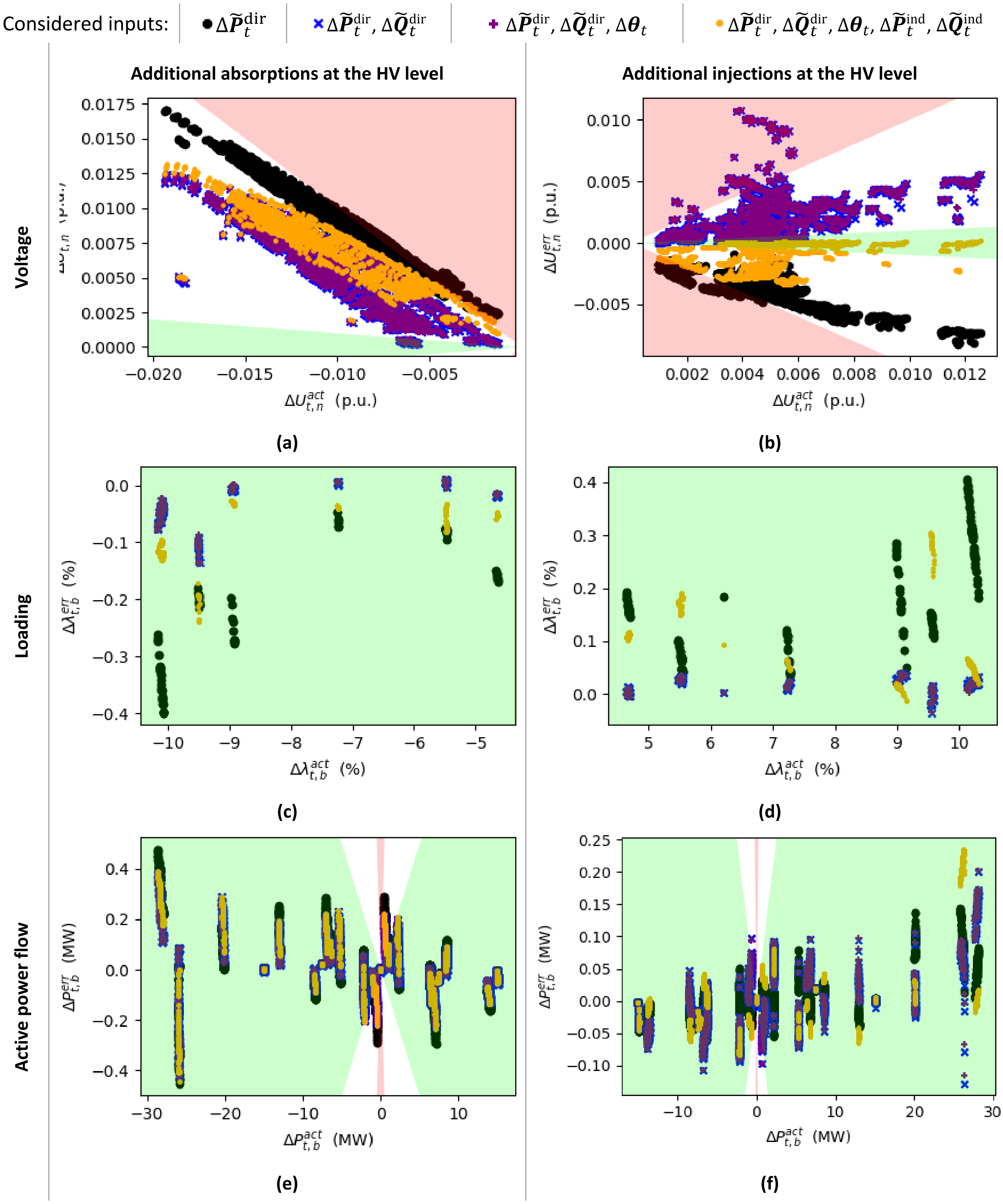

Figure 10: Absolute estimation errors for all relevant elements, time intervals, and additional absorptions / injections at the HV level: (a) voltage errors for absorptions; (b) voltage errors for injections; (c) loading errors for absorptions; (d) loading errors for injections; (e) active power errors for absorptions; (f) active power errors for injections. Voltage and loading errors are plotted only for the critical elements, and the active power flows are plotted for all branches. Areas with relative errors above 100 % and below 10 % are marked by red and green backgrounds, respectively. Different markers show which model inputs are considered: black dot → direct active power changes; blue x → direct power changes; purple plus → tap position and direct power changes; yellow dot → all inputs.

4.2.4. Result discussion

The simplified distribution system model does not appropriately reflect the responses of distribution system controls to flexibility activations; they must be provided as model inputs or neglected. Simulation results indicate relatively good performance of loading and active power flow estimation, even when control responses are neglected. Meanwhile, a significant impact of the control responses on the voltage estimation accuracy is observed: The individual neglection of $Q(U)$-controls and on-load tap changers provokes considerable voltage estimation errors at the 20 kV level. However, their errors partly compensate each other when both control types are simultaneously neglected. This compensating effect is absent at the 110 kV level: The $Q(U)$ controls but not the 110/20 kV on-load tap changers have significant impact on the voltage estimation accuracy. Here, relative high errors occur in some cases even when all control responses are perfectly known and considered.

4.3. Process pre-validation

The core functionalities of the planned DSO/TSO interaction process are simulated to provide insights into the suitability of the optimization problem formulation and the NSGA2 algorithm to solve this problem.

4.3.1. Test system description

The pre-validation requires a baseline scenario and a bid scenario. The baseline scenario is similar[7] to the one described in section 4.2.1.1, except that four industrial customers are added to the 110 kV grid and seven ones to the 20 kV network. Their load profiles and redispatch bids are synthesized by the bid generator. An overview of all bids and their detailed time-curves are given in Table 9 and Figure 17 to Figure 27 in the annex. No contingency cases are considered but only the case without any contingencies (all lines and transformers are in service).

4.3.2. Evaluation methodology

The detailed distribution system model described in section 4.3.1 is used to calculate the parameters of the simplified model [Eq. (2.17)] as defined in section 3.1.1.1. The optimization objectives and constraints formulated in Eq. (3.2) are determined by solving the optimization problem with the NSGA2 algorithm and by simulating and estimating the network state for all relevant bid combinations according to the brute-force approach. The simulation and estimation results are compared with each other to analyze the suitability of the optimization constraint formulation based on four evaluation criteria:

1. False approval rate:
   Share of bid sets that are erroneously approved, i.e., only the simulated but not the estimated values violate their limits.
2. False rejection rate:
   Share of bid sets that are erroneously rejected, i.e., only the estimated but not the simulated values violate their limits.
3. Correct approval rate:
   Share of bid sets that are correctly approved, i.e., both the simulated and estimated values do not violate their limits.
4. Correct rejection rate:
   Share of bid sets that are correctly rejected, i.e., both the simulated and estimated values violate their limits.

All nodes and branches whose simulated voltages and loadings violate their limits for at least one bid set are regarded as critical. The estimation absolute errors are calculated for the critical elements as in Eq. (4.2)

4.3.3. Evaluation results

4.3.3.1. Baseline network state

We analyze the baseline network state of the test distribution system, i.e., the voltages of all nodes and the loadings of all branches without any activated bids [Figure 11]. The baseline network state is critical (at the MV level) but does not violate any limits. The lower voltage level is almost violated at 07:15 and 16:00, reaching minimum voltage values

[7] sb-code: “1-HVMV-mixed-1.105-0-no_sw”; scenario: “hPV”.

of 0.9673 and 0.9706 p.u. [see Figure 11a]. The upper loading limit is approached at 08:00 with a maximum value of 94.21 %.

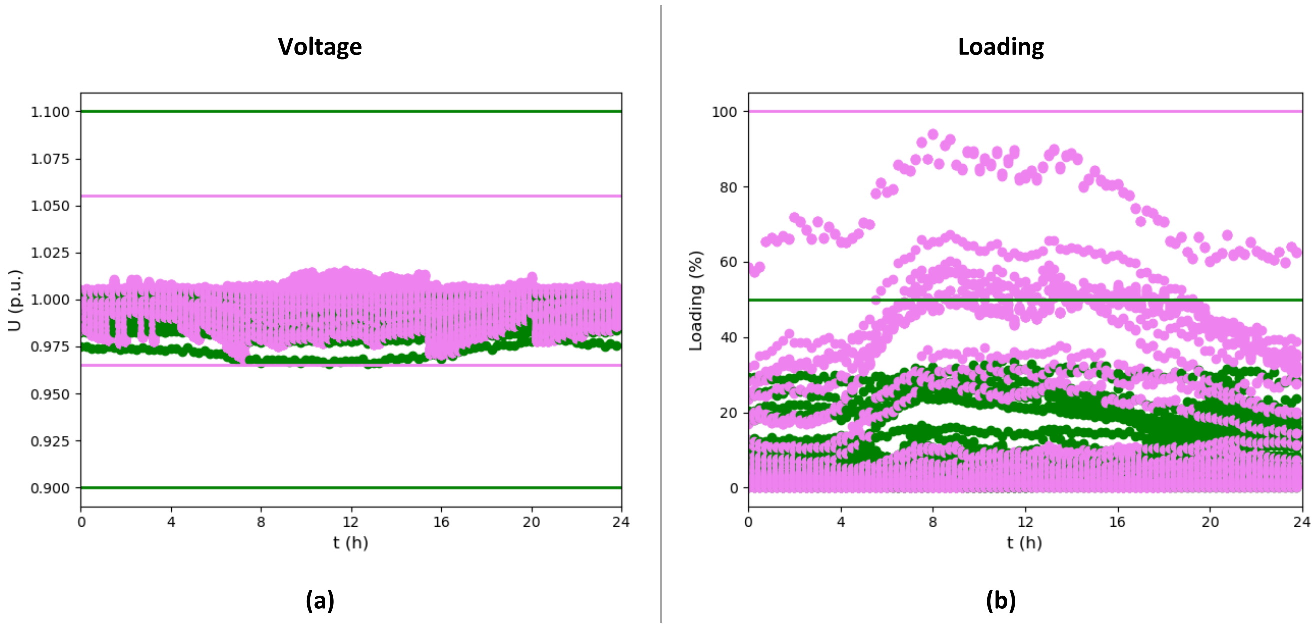

Figure 11: Baseline state of the test distribution network: (a) node voltages; (b) branch loadings. Purple dots mark voltage and loadings at the MV level and green ones refer to the HV level. The limits are shown in the respective colors.

4.3.3.2. Voltage estimation errors

Here, we investigate the voltage estimation errors resulting from the use of the simplified DS model for all bid sets [Figure 12]. Most voltages are estimated with a relative error of about 100 %, reaching, for instance, an absolute value of 0.01609 p.u. for an actual voltage change of 0.01594 p.u.

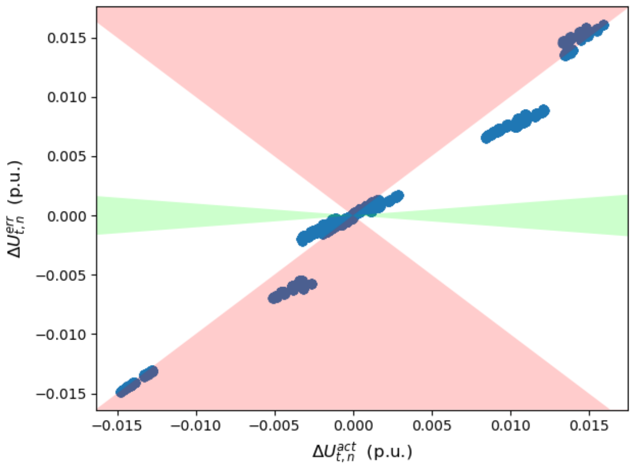

Figure 12: Voltage estimation errors for critical nodes. Areas with relative errors above 100 % and below 10 % are marked by red and green backgrounds, respectively.

4.3.3.3. Margins and decision rates

The process described in section 3 uses the simplified DS model to reject infeasible bid sets, i.e., bid sets that provoke violations of the operational distribution network limits. The inaccuracies introduced by this model (see section 4.3.3.2) may lead to false bid set approvals, i.e., approvals of infeasible bid sets. Such false approvals are inacceptable, and therefore, must be avoided in any case. A suitable approach to avoid these false approvals is to use tightened limits in the formulation of the optimization problem, i.e., for bid set filtering.

Table 5 introduces safety margins for the lower voltage limit that ensure the reliable identification of infeasible bid sets. The optimal margin of 0.004 p.u., which corresponds to a lower voltage limit of 0.969 p.u., is the lowest value that removes all false approvals. This value (which is obtained from the simulation and estimation results) is unknown during process execution, and therefore, must be estimated conservatively enough to remove all false approvals. A conservative safety margin of 0.009 p.u. is used in the following analysis.

Table 5: Operational limits of the test distribution system for different margins.

Margins	Level	Lower voltage limit (p.u.)	Upper voltage limit (p.u.)	Upper loading limit (%)
None	20 kV	0.965	1.055	100
	110 kV	0.900	1.100	50
Optimal	20 kV	0.969	1.055	100
	110 kV	0.900	1.100	50
Conservative	20 kV	0.974	1.055	100
	110 kV	0.900	1.100	50

Table 6 lists the decision rates of the simplified DS model for several margins. Without any additional safety margin, not a single bid set is falsely rejected. However, 16.67 % of all bid sets are wrongly approved, which is inacceptable. Using the optimal safety margin removes all false approvals but causes 81.48 % of all bid sets to be erroneously rejected. The conservative margin increases this false rejection rate even to 82.92 %.

Table 6: Decision rates of the simplified DS model for different margins.

Margins	False rejection (%)	False approval (%)	Corr. rejection (%)	Corr. approval (%)	False decision (%)
None	0.0	16.67	0.0	83.33	16.67
Optimal	81.48	0.0	16.67	1.85	81.48
Conservative	82.92	0.0	16.67	0.41	82.92

Guessing whether the bid sets provoke limit violations would yield a false decision rate around 50 %, but false approvals might be included in the guess.

4.3.3.4. Objectives

This section analyzes – for different time points and margins from Table 5 – the objectives and constraints for all bid sets calculated by optimization, brute-force simulation, and brute-force estimation according to Eq. (2.15) and (2.17) [Figure 13]. All bid sets have the same costs and almost the same active power values for both DS models, only the compliance with the constraints is differently evaluated. Results show that – in accordance with Table 6 – the number of false decisions is much higher when margins are used.

Despite the false approval rate of 16.67 % – the simplified DS model and the NSGA2 algorithm correctly identify the pareto front at 9:00 when no margins are used [Figure 13a]. Meanwhile, at 14:45, two bid sets within the pareto front are erroneously approved (including “bid set 2”) [Figure 13b]. Here, the NSGA2 algorithm finds the same pareto front as the brute-force calculation based on the simplified DS model.

Using margins drastically increases the false rejection rate (see Table 6), and consequently, the estimated pareto front greatly differs from the simulated one. The low numbers of approved bid sets (1.85 % and 0.41 %) make it difficult to solve the optimization problem, and consequently, the NSGA2 algorithm does not find any solution. When optimal margins are used, only a few pareto optimal bid sets with very low active power are approved at 9:00 while the ones with high power are erroneously rejected [Figure 13c]. At 14:45, none of the optimal bid sets are identified through estimations [Figure 13d]. Unnecessary cost increases and the loss of bid sets with high power are the consequence.

As the decision rates are quite similar for the optimal and conservative margins, the same pareto fronts are found in both cases [compare Figure 13c-d with Figure 13e-f].

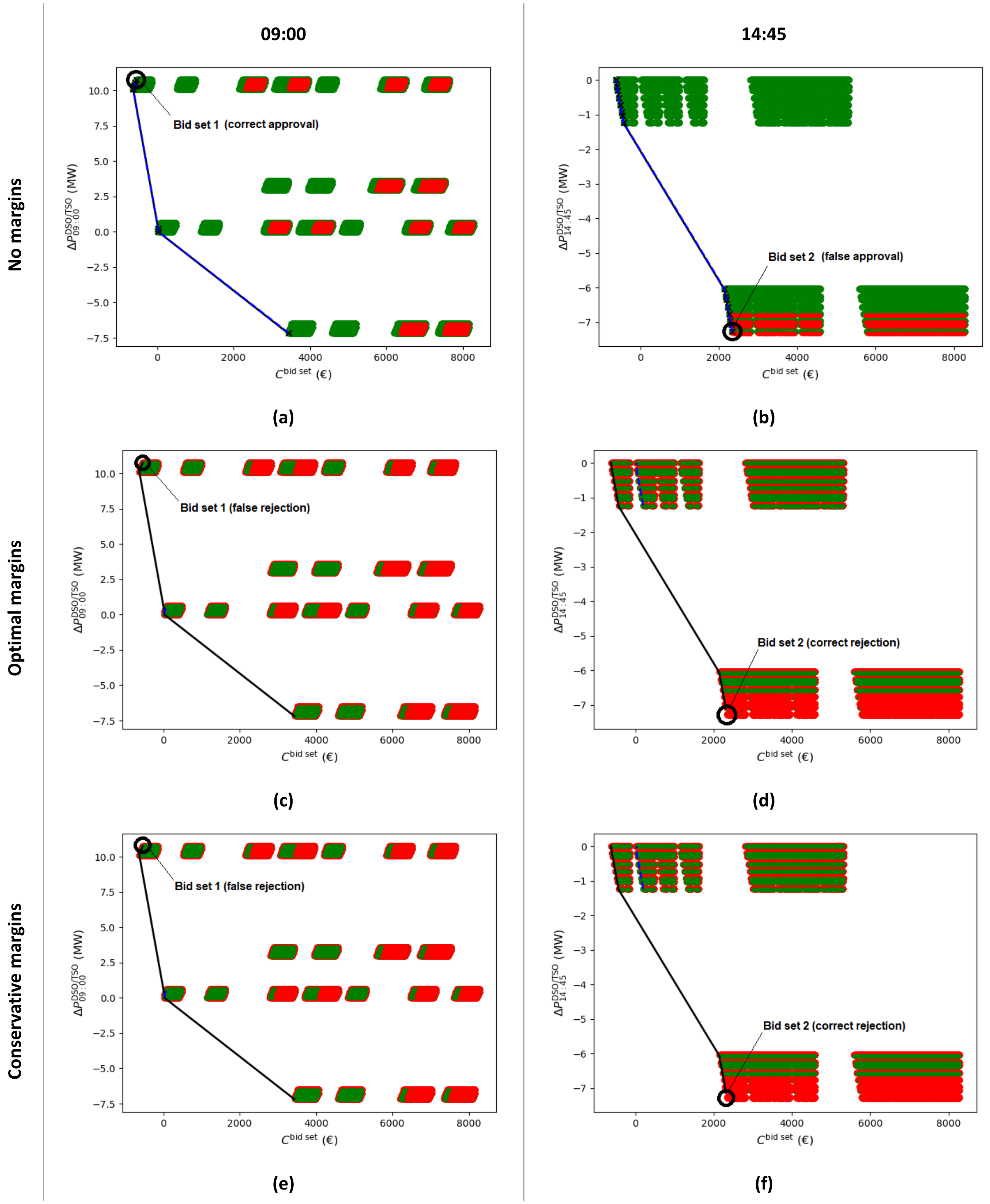

Figure 13: Optimization objectives and constraints of all bid sets for different time intervals and margins: (a) 09:00, no margins; (b) 14:45, no margins; (c) 09:00, optimal margins; (d) 14:45, optimal margins; (e) 09:00, conservative margins; (f) 14:45, conservative margins. Different markers show how the results are calculated: crosses → optimization; small dots → brute force simulation; large dots → brute force estimation. Green dots indicate that no limit violations are detected by the underlying model and red dots indicate that limit violations are detected. The black solid and blue dashed lines show the pareto fronts resulting from the detailed and simplified DS model, respectively. The two bid sets marked by black circles and denoted as "bid set 1" and "bid set 2" are further analyzed in section 4.3.3.5.

4.3.3.5. Voltage profiles

This section analyzes the voltage profiles of the 20 kV feeders to reveal the reasons for the decisions made by the optimizer or simplified DS model for selected cases.

First, we analyze the effects of “bid set 1” at 9:00 and 7:15 [Figure 14]. It is correctly approved when no margins are used and erroneously rejected when margins are used. At 9:00, three low power bids (3 x 0.2 MW injection) are activated at the MV level and one high power bid (1 x 10 MW injection) at the HV level [Figure 14a]. The baseline tap position and the one resulting from the activation of “bid set 1” are both -5, which means that the bid set activation does not provoke a reaction of the tap changer. The voltage increase due to the additional injections at the MV level are underestimated by the simplified DS model. However, neither the simulated nor the estimated voltages fall below any limit, and consequently, the bid set would be approved if only this single time point would be considered for bid set filtering (which is not the case, see Eq. (4.3c-e)). The reason why “bid set 1” is erroneously rejected when margins are used occurs at 07:15 [Figure 14b]. At this time, no bids are active at the MV but only at the HV level (1 x 10 MW injection). Again, the bid set activation does not lead to a tap reaction (both baseline and calculated tap positions are -4). As the additional injection at the HV level has low effect on MV feeder voltages, the baseline, estimated, and calculated voltage profiles are almost equal. In this case, the estimated voltages violate the conservative and optimal limits, while the calculated voltages do not violate their actual limit.

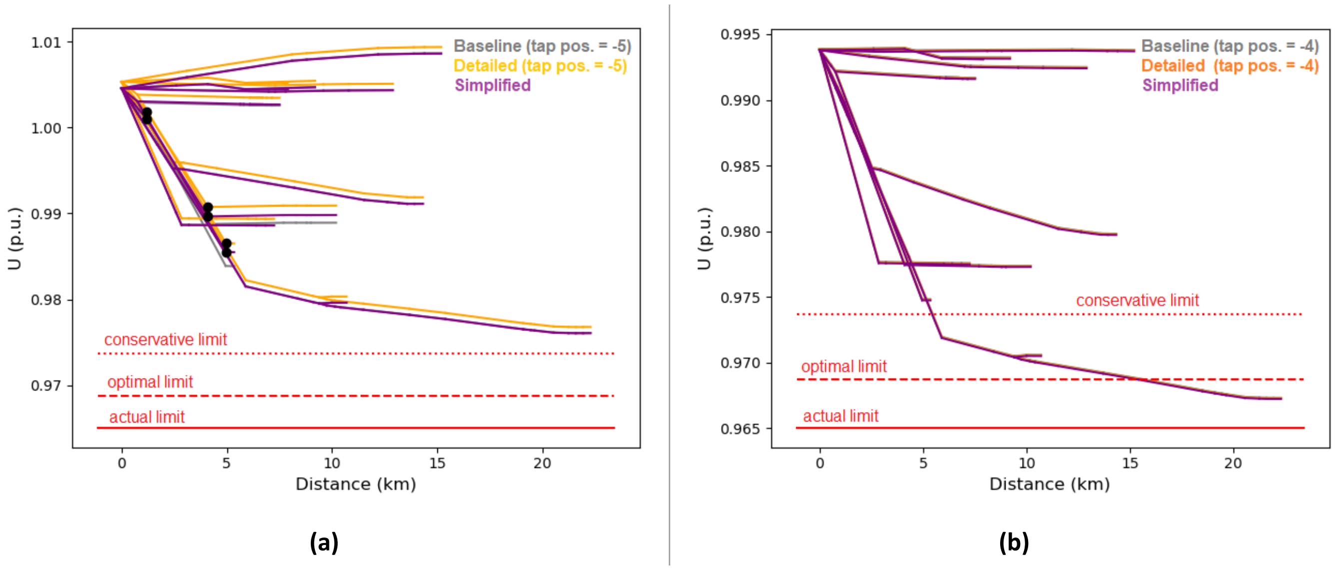

Figure 14: Voltage profiles of the 20 kV feeders for “bid set 1” and different time points: (a) 09:00; (b) 07:15. Baseline values are shown in gray, and the simulated and estimated values resulting from the activation of “bid set 1” are shown in orange and purple, respectively. Red lines show the lower voltage limits listed in Table 5. The positions of the industries whose bids are currently activated are marked by black filled circles.

Now, we analyze the effects of “bid set 2” at 13:00 and 16:00 [Figure 15]. It is erroneously approved when no margins are used and correctly rejected if margins are applied. At 13:00, four bids (6 MW, 0.7 MW, 0.3 MW, and 0.2 MW absorptions) are active at the MV level, and none at the HV level [Figure 15a]. The activation of this bid set does not provoke a reaction of the tap changer at 13:00. Again, the simplified DS model underestimates the voltage decreasing effect of the additional consumption. The calculated voltages violate their actual lower limit, and the estimated ones violate the conservative but not the optimal limit. However, at 16:00, when only one bid is active (6 MW consumption), the estimated voltages violate their optimal limit [Figure 15b], leading to a correct rejection of the bid set. Simulation results show that the activation of “bid set 2” provokes a shift of the tap position at 16:00, leading to increased voltages. This effect is not reflected by the simplified DS model, which yields decreased voltages instead of increased ones.

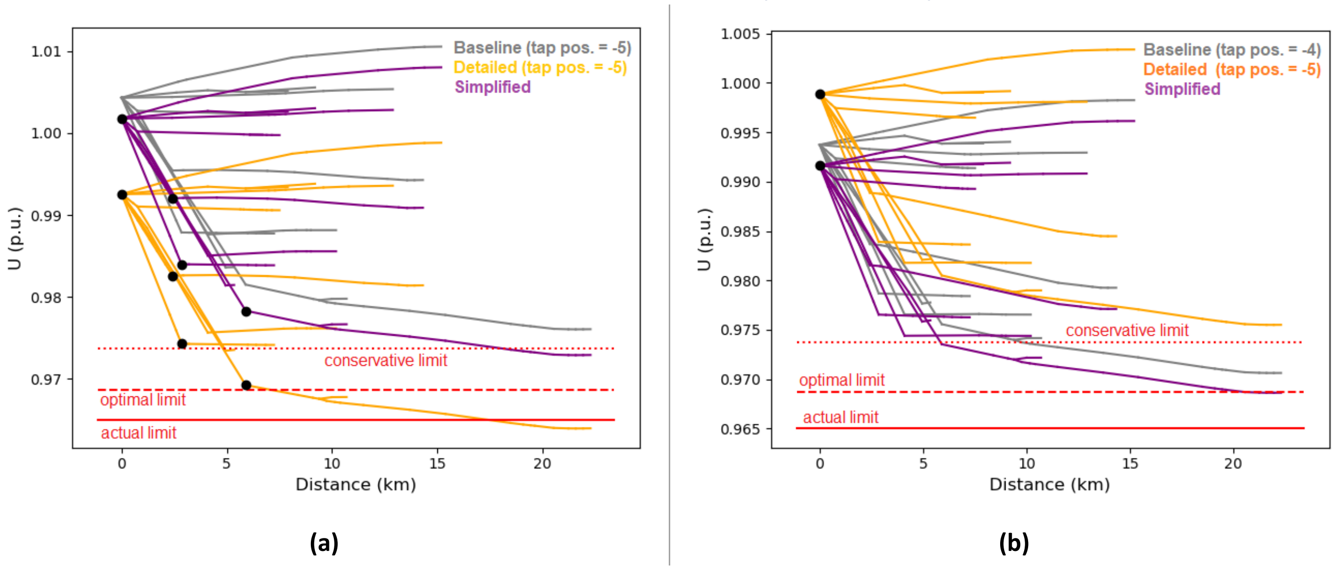

Figure 15: Voltage profiles of the 20 kV feeders for "bid set 2" and different time points: (a) 13:00; (b) 16:00. Baseline values are shown in gray, and the simulated and estimated values resulting from the activation of "bid set 1" are shown in orange and purple, respectively. Red lines show the lower voltage limits listed in Table 5. The positions of the industries whose bids are currently activated are marked by black filled circles.

4.3.4. Result discussion

The presented simulation results provide deep insights concerning the suitability of the optimization problem formulation and the NSGA2 algorithm.

The problem formulation based on the simplified DS model introduces severe inaccuracies in voltage estimation due to the non-linear character of distribution systems. The network-related non-linearities lead to an underestimation of the voltage changes that result from bid set activation. This underestimation may lead to an erroneous approval of infeasible bid sets, which is inacceptable. Such false approvals can be avoided by using safety margins, i.e., by using tightened voltage limits in the optimization problem formulation. If these safety margins are appropriately set, they prevent false approvals but simultaneously increase the false rejection rate. However, the inability of the simplified DS model to consider on-load tap changers may lead to completely wrong voltage estimations, i.e., it may yield decreased voltages although voltages are increasing and vice versa. False decision rates from 16.67 % (no margins) and 82.92 % (conservative margins) are observed in the simulated example. The cases with no and optimal margins have no practical relevance, as falsely approved bid sets are inacceptable, and the optimal margins are unknown during process execution. The high false rejection rate resulting from the use of conservative margins reduces the amount of active power available for redispatch at the transmission level and increase redispatch costs.

In general, the result of an optimization algorithm can only be as good as the underlying problem formulation or model. The NSGA2 algorithm reliably finds the same pareto front as the brute-force estimations for all bid sets when no margins are applied. However, the algorithm does not find any solution in the analyzed example when margins are applied and – in further consequence – only very few bid sets (0.41 % and 1.85 %) satisfy the optimization constraints.

5. Conclusions

This deliverable presents and pre-validates the final process specification for the planned DSO/TSO interaction; the simulation environment used for pre-validation is overviewed.

The developed simulation environment enables an in-depth analysis of the planned interaction process by facilitating scenario definition, process simulation, and process evaluation. Its ability to calculate the distribution network state for large numbers of bid sets allows analyzing the formulated optimization problem and the chosen solver algorithm.

The linearized distribution system model enables a slim problem formulation that preserves the privacy of DSOs and promotes transparent bid set filtering while degrading calculation accuracy. Simulation results underline its ability to accurately estimate the effects of bid set activations on the loading of critical branches and the active power exchanges between the DSO and TSO. However, they also reveal severe inaccuracies in voltage estimations, which are necessary to consider the upper and lower voltage limits of distribution networks in bid set filtering.

The process pre-validation results show that the optimization problem formulation does not guarantee the rejection of all infeasible bid sets if the actual voltage limits of the distribution network are used. Using tightened limits removes all false approvals but increases the number of false rejections, leading to a false rejection rate of 82.92 % in the analyzed example. These false rejections reduce the power available for redispatch at the transmission level and increases the redispatch costs. The NSGA2 algorithm identifies the correct pareto front when no margins are applied to the investigated example, but when margins are applied and only a few bid sets remain that satisfy the optimization constraints, it does not find any solution.

As the false decision rate is very sensitive to the underlying scenario, a comprehensive scalability analysis is necessary to evaluate the applicability of the planned interaction process under various conditions. This analysis, which is conducted in WP8 of this project, should systematically investigate scenarios that are critical for the upper and lower voltage limits and the loading limits at both the high and medium voltage levels.

6. References

[1] A. Arif, Z. Wang, J. Wang, B. Mather, H. Bashualdo, and D. Zhao, “Load Modeling—A Review,” *IEEE Transactions on Smart Grid*, vol. 9, no. 6, pp. 5986–5999, Nov. 2018, doi: 10.1109/TSG.2017.2700436.

[2] O. Marggraf *et al.*, “U-Control - Analysis of Distributed and Automated Voltage Control in current and future Distribution Grids,” in *International ETG Congress 2017*, Nov. 2017, pp. 1–6.

[3] J. Blank and K. Deb, “Pymoo: Multi-Objective Optimization in Python,” *IEEE Access*, vol. 8, pp. 89497–89509, 2020, doi: 10.1109/ACCESS.2020.2990567.

[4] “pymoo - NSGA-II: Non-dominated Sorting Genetic Algorithm.” Accessed: Jul. 18, 2023. [Online]. Available: https://pymoo.org/algorithms/moo/nsga2.html#nb-nsga2

[5] “EDI Library.” Accessed: Oct. 10, 2023. [Online]. Available: https://www.entsoe.eu/publications/electronic-data-interchange-edi-library/

[6] “PowerFactory - DIgSILENT.” Accessed: Aug. 07, 2023. [Online]. Available: https://www.digsilent.de/en/powerfactory.html

[7] “Welcome to Python.org,” Python.org. Accessed: Aug. 07, 2023. [Online]. Available: https://www.python.org/

[8] S. Meinecke *et al.*, “SimBench—A Benchmark Dataset of Electric Power Systems to Compare Innovative Solutions Based on Power Flow Analysis,” *Energies*, vol. 13, no. 12, Art. no. 12, Jan. 2020, doi: 10.3390/en13123290.

[9] D.-L. Schultis, “Accuracy Analysis of a Sensitivity-Based Distribution System Model for the Centralized Redispatch of Distributed Flexibilities,” presented at the 27th International Conference on Electricity Distribution, Rome, Italy, Jun. 2023, p. 10637.

[10] D.-L. Schultis and A. Ilo, “Increasing the Utilization of Existing Infrastructures by Using the Newly Introduced Boundary Voltage Limits,” *Energies*, vol. 14, no. 16, Art. no. 16, Jan. 2021, doi: 10.3390/en14165106.

[11] D.-L. Schultis, S. Petrusic, and A. Ilo, “Modelling of low-voltage grids with high PV share and Q(U)-control,” *CIRED - Open Access Proceedings Journal*, vol. 2020, no. 1, pp. 501–504, Apr. 2021, doi: 10.1049/oap-cired.2021.0101.

Annex

Equation (A1) defines the sensitivity matrices used in Equation (2.16) and (2.17), which are associated to an arbitrary time interval.

$$J_{m,t}^{P/P} = \begin{bmatrix} \frac{\partial P_{m,t,1}}{\partial \tilde{P}_{m,t,1}} & \cdots & \frac{\partial P_{m,t,1}}{\partial \tilde{P}_{m,t,L}} \\ \vdots & \ddots & \vdots \\ \frac{\partial P_{m,t,B}}{\partial \tilde{P}_{m,t,1}} & \cdots & \frac{\partial P_{m,t,B}}{\partial \tilde{P}_{m,t,L}} \end{bmatrix} \quad J_{m,t}^{U/P} = \begin{bmatrix} \frac{\partial U_{m,t,1}}{\partial \tilde{P}_{m,t,1}} & \cdots & \frac{\partial U_{m,t,1}}{\partial \tilde{P}_{m,t,L}} \\ \vdots & \ddots & \vdots \\ \frac{\partial U_{m,t,N}}{\partial \tilde{P}_{m,t,1}} & \cdots & \frac{\partial U_{m,t,N}}{\partial \tilde{P}_{m,t,L}} \end{bmatrix} \quad J_{m,t}^{\lambda/P} = \begin{bmatrix} \frac{\partial \lambda_{m,t,1}}{\partial \tilde{P}_{m,t,1}} & \cdots & \frac{\partial \lambda_{m,t,1}}{\partial \tilde{P}_{m,t,L}} \\ \vdots & \ddots & \vdots \\ \frac{\partial \lambda_{m,t,B}}{\partial \tilde{P}_{m,t,1}} & \cdots & \frac{\partial \lambda_{m,t,B}}{\partial \tilde{P}_{m,t,L}} \end{bmatrix} \quad \text{(A1a)}$$

$$J_{m,t}^{P/Q} = \begin{bmatrix} \frac{\partial P_{m,t,1}}{\partial \tilde{Q}_{m,t,1}} & \cdots & \frac{\partial P_{m,t,1}}{\partial \tilde{Q}_{m,t,L}} \\ \vdots & \ddots & \vdots \\ \frac{\partial P_{m,t,B}}{\partial \tilde{Q}_{m,t,1}} & \cdots & \frac{\partial P_{m,t,B}}{\partial \tilde{Q}_{m,t,L}} \end{bmatrix} \quad J_{m,t}^{U/Q} = \begin{bmatrix} \frac{\partial U_{m,t,1}}{\partial \tilde{Q}_{m,t,1}} & \cdots & \frac{\partial U_{m,t,1}}{\partial \tilde{Q}_{m,t,L}} \\ \vdots & \ddots & \vdots \\ \frac{\partial U_{m,t,N}}{\partial \tilde{Q}_{m,t,1}} & \cdots & \frac{\partial U_{m,t,N}}{\partial \tilde{Q}_{m,t,L}} \end{bmatrix} \quad J_{m,t}^{\lambda/Q} = \begin{bmatrix} \frac{\partial \lambda_{m,t,1}}{\partial \tilde{Q}_{m,t,1}} & \cdots & \frac{\partial \lambda_{m,t,1}}{\partial \tilde{Q}_{m,t,L}} \\ \vdots & \ddots & \vdots \\ \frac{\partial \lambda_{m,t,B}}{\partial \tilde{Q}_{m,t,1}} & \cdots & \frac{\partial \lambda_{m,t,B}}{\partial \tilde{Q}_{m,t,L}} \end{bmatrix} \quad \text{(A1b)}$$

$$J_{m,t}^{P/\theta} = \begin{bmatrix} \frac{\partial P_{m,t,1}}{\partial \theta_{m,t,1}} & \cdots & \frac{\partial P_{m,t,1}}{\partial \theta_{m,t,\rho}} \\ \vdots & \ddots & \vdots \\ \frac{\partial P_{m,t,B}}{\partial \theta_{m,t,1}} & \cdots & \frac{\partial P_{m,t,B}}{\partial \theta_{m,t,\rho}} \end{bmatrix} \quad J_{m,t}^{U/\theta} = \begin{bmatrix} \frac{\partial U_{m,t,1}}{\partial \theta_{m,t,1}} & \cdots & \frac{\partial U_{m,t,1}}{\partial \theta_{m,t,\rho}} \\ \vdots & \ddots & \vdots \\ \frac{\partial U_{m,t,N}}{\partial \theta_{m,t,1}} & \cdots & \frac{\partial U_{m,t,N}}{\partial \theta_{m,t,\rho}} \end{bmatrix} \quad J_{m,t}^{\lambda/\theta} = \begin{bmatrix} \frac{\partial \lambda_{m,t,1}}{\partial \theta_{m,t,1}} & \cdots & \frac{\partial \lambda_{m,t,1}}{\partial \theta_{m,t,\rho}} \\ \vdots & \ddots & \vdots \\ \frac{\partial \lambda_{m,t,B}}{\partial \theta_{m,t,1}} & \cdots & \frac{\partial \lambda_{m,t,B}}{\partial \theta_{m,t,\rho}} \end{bmatrix} \quad \text{(A1c)}$$

Table 7 shows the parametrization of the NSGA2 algorithm used to solve the optimization problem according to Eq. (3.3). The default values are used for the remaining parameters.

Table 7: Parametrization of the NSGA2 algorithm provided by pymoo.

Parameter	Value
pop_size	100
sampling	Binary random sampling
crossover	Two-point crossover
mutation	Bit flip mutation
eliminate_duplicates	True

Figure 16 and Table 8 provide the $Q(U)$ control parameters used for all simulations. S_r is the inverter rating.

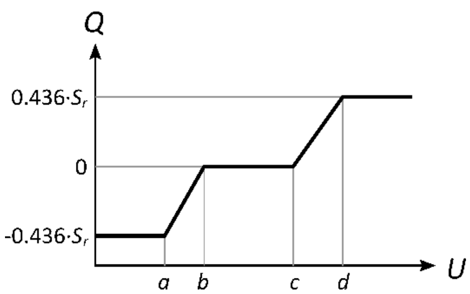

Figure 16: Generic Q(U) control characteristic.

Table 8: Q(U) control parameters used for all simulations.

Parameter	LV level	MV level	HV level
a	0.92 p.u.	0.95 p.u.	0.95 p.u.
b	0.96 p.u.	0.99 p.u.	0.99 p.u.
c	1.05 p.u.	1.01 p.u.	1.01 p.u.
d	1.08 p.u.	1.04 p.u.	1.04 p.u.

Table 9 overviews the industry bids used for the Process pre-validation conducted in section 4.3; their detailed time-curves are shown in Figure 17 to Figure 27 (positive power means reduced consumption).

Table 9: Overview of industry bids.

Industry ID	Industry sector	Level	Bid ID	Bid energy (MWh)	Maximal bid power (MW)	Catch-up effect	IDs of XOR-linked bids
Ind_1	Food	MV	1	0.4	0.2	Yes	2
			2	0.4	0.2	Yes	1
Ind_2	Food	MV	3	0.6	0.3	Yes	4
			4	0.6	0.3	Yes	3
Ind_3	Chemistry	MV	5	0.4	0.2	Yes	6
			6	0.4	0.2	Yes	5
Ind_4	Paper	HV	7	30	10	No	-
Ind_5	Chemistry	MV	8	1.4	0.7	Yes	9
			9	1.4	0.7	Yes	8
Ind_6	Paper	HV	10	42	7	No	11, 12
			11	42	7	No	10, 12
			12	42	7	No	10, 11
Ind_7	Cement	HV	13	36	6	No	14, 15
			14	36	6	No	13, 15
			15	36	6	No	13, 14
Ind_8	Paper	HV	16	0.825	0.3	No	-
Ind_9	Food	MV	17	0.4	0.2	Yes	18
			18	0.4	0.2	Yes	17
Ind_10	Paper	HV	19	6	2	No	-
Ind_11	Chemistry	MV	20	0.4	0.2	Yes	21
			21	0.4	0.2	Yes	20

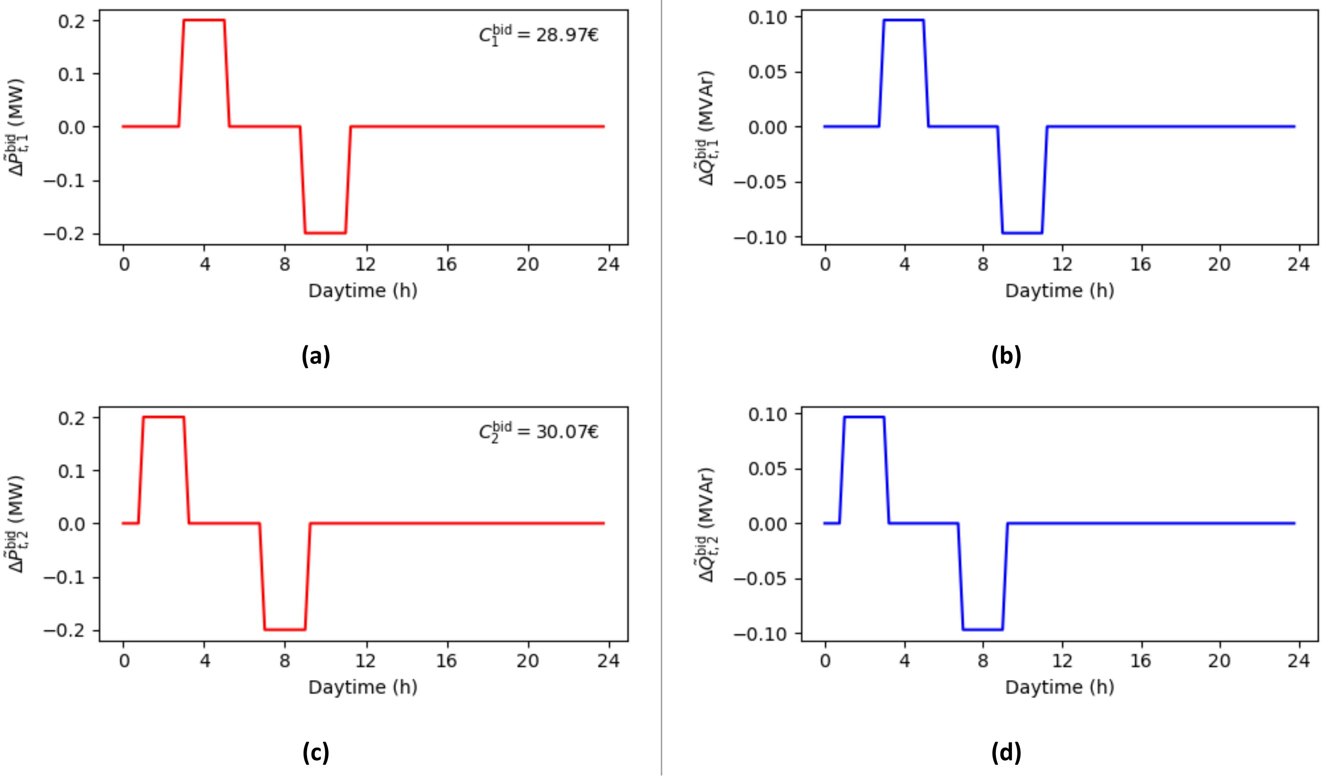

Figure 17: Bids and the associated direct reactive power changes of industry 'Ind_1': (a, b) Bid with ID 1; (c, d) Bid with ID 2.

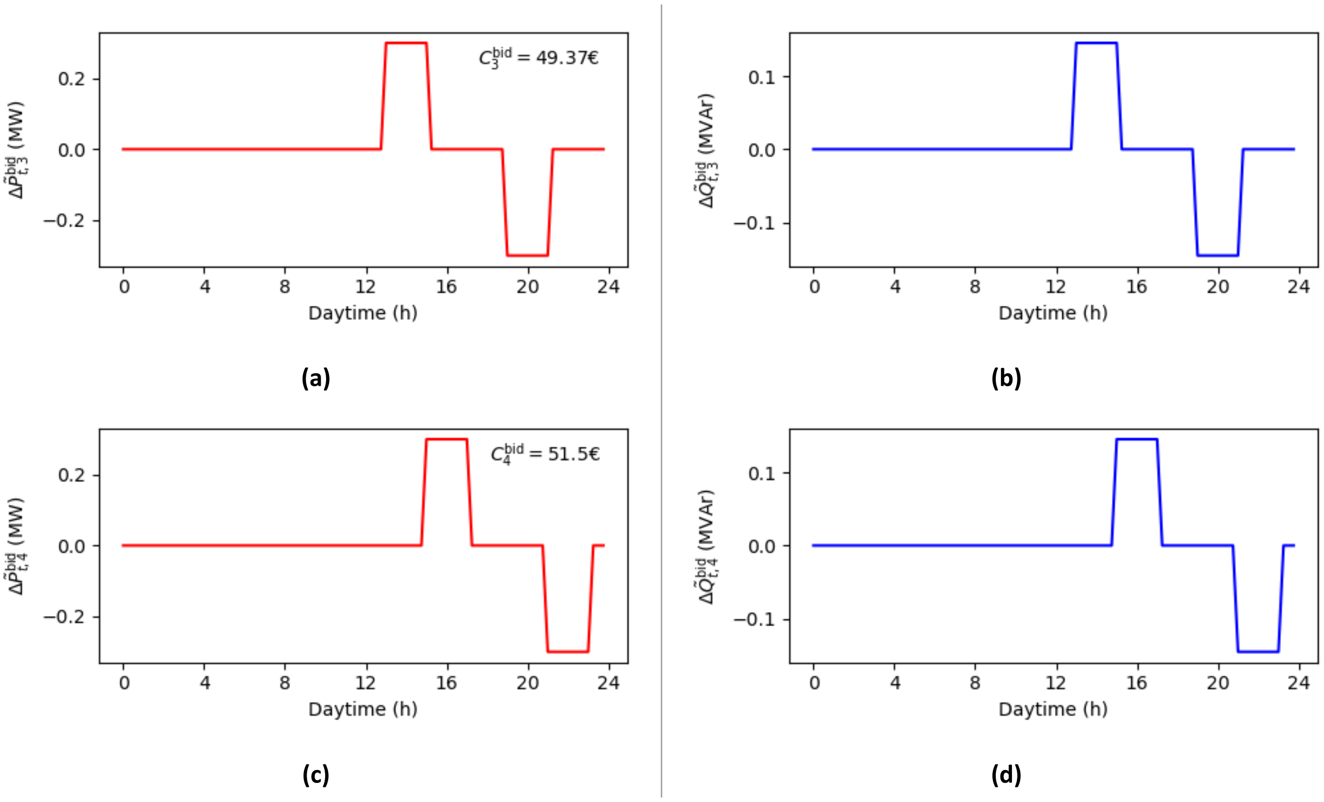

Figure 18: Bids and the associated direct reactive power changes of industry 'Ind_2': (a, b) Bid with ID 3; (c, d) Bid with ID 4.

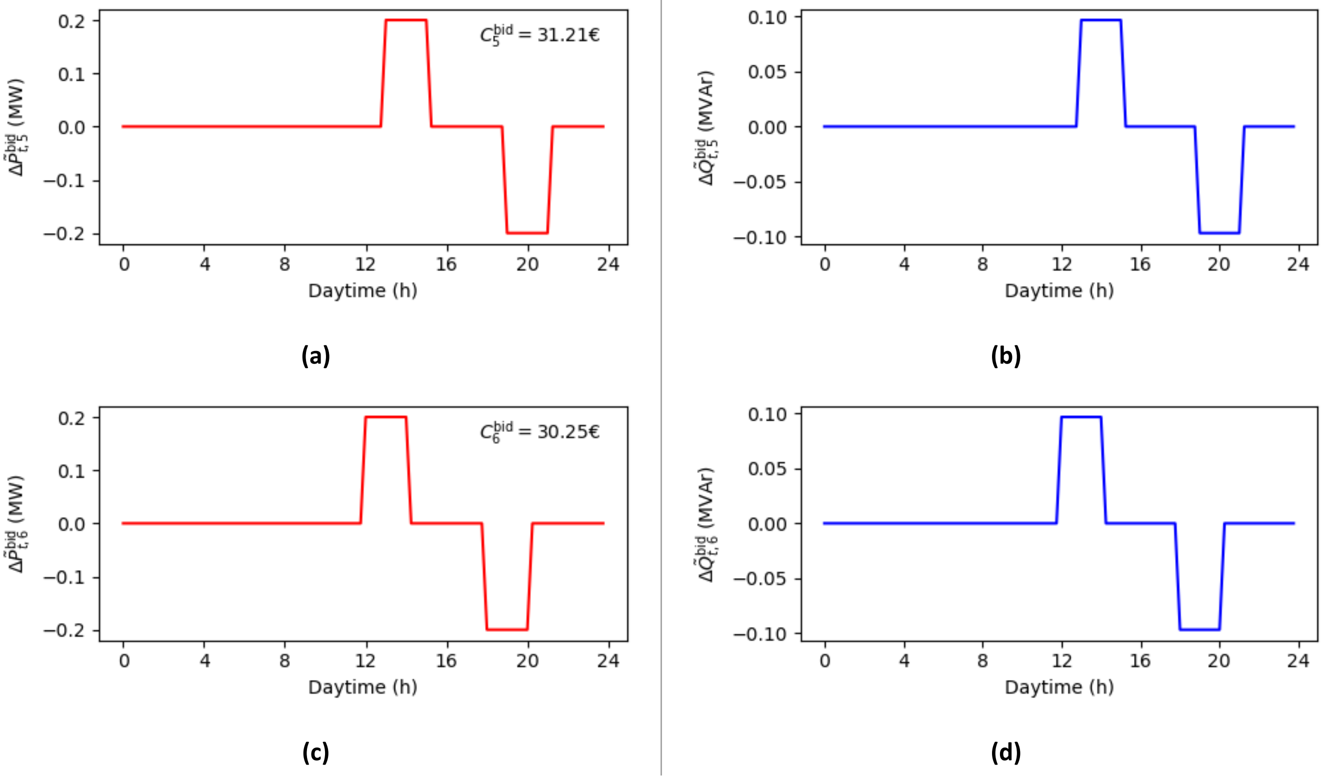

Figure 19: Bids and the associated direct reactive power changes of industry 'Ind_3': (a, b) Bid with ID 5; (c, d) Bid with ID 6.

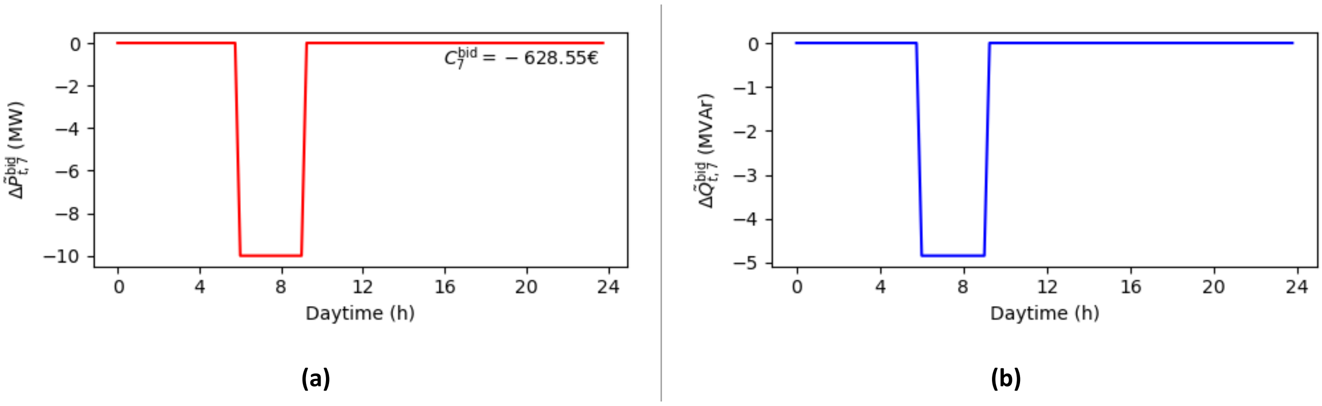

Figure 20: Bids and the associated direct reactive power changes of industry 'Ind_4': (a, b) Bid with ID 7.

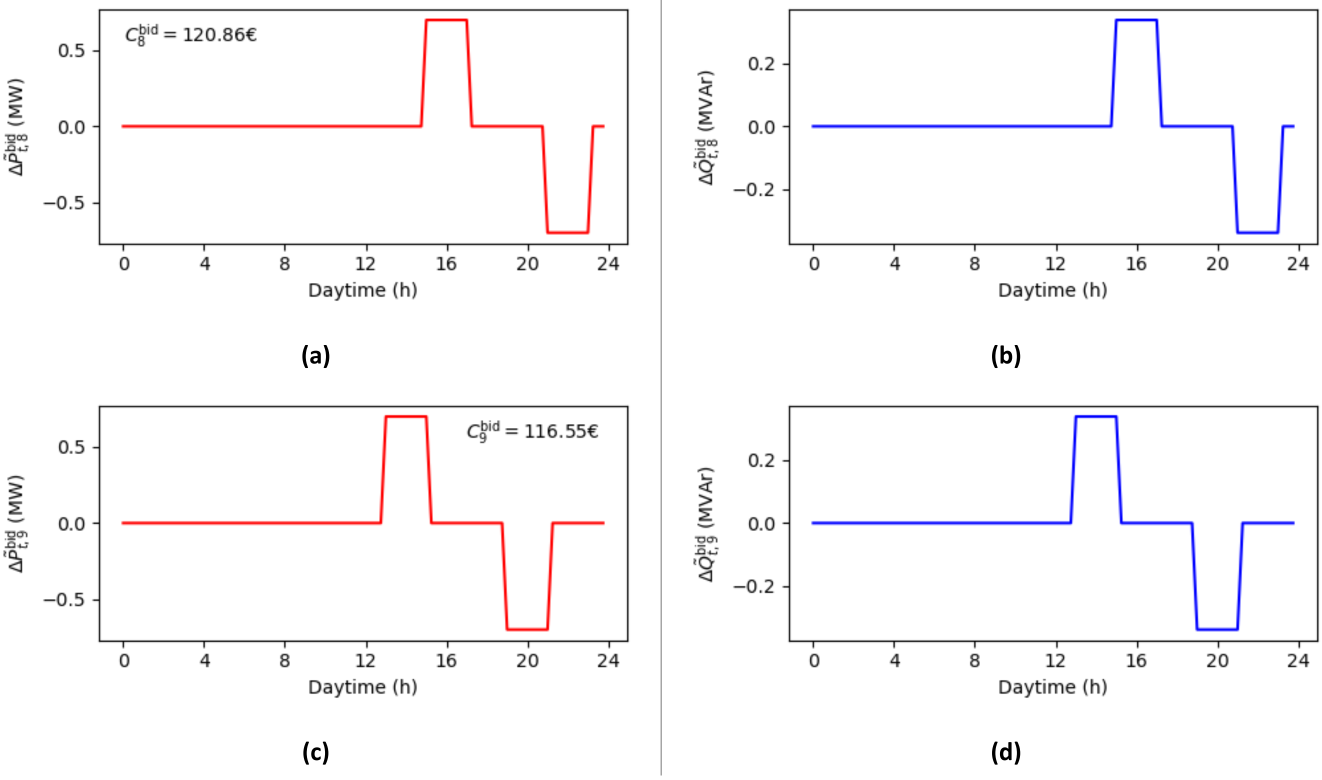

Figure 21: Bids and the associated direct reactive power changes of industry 'Ind_5': (a, b) Bid with ID 8; (c, d) Bid with ID 9.

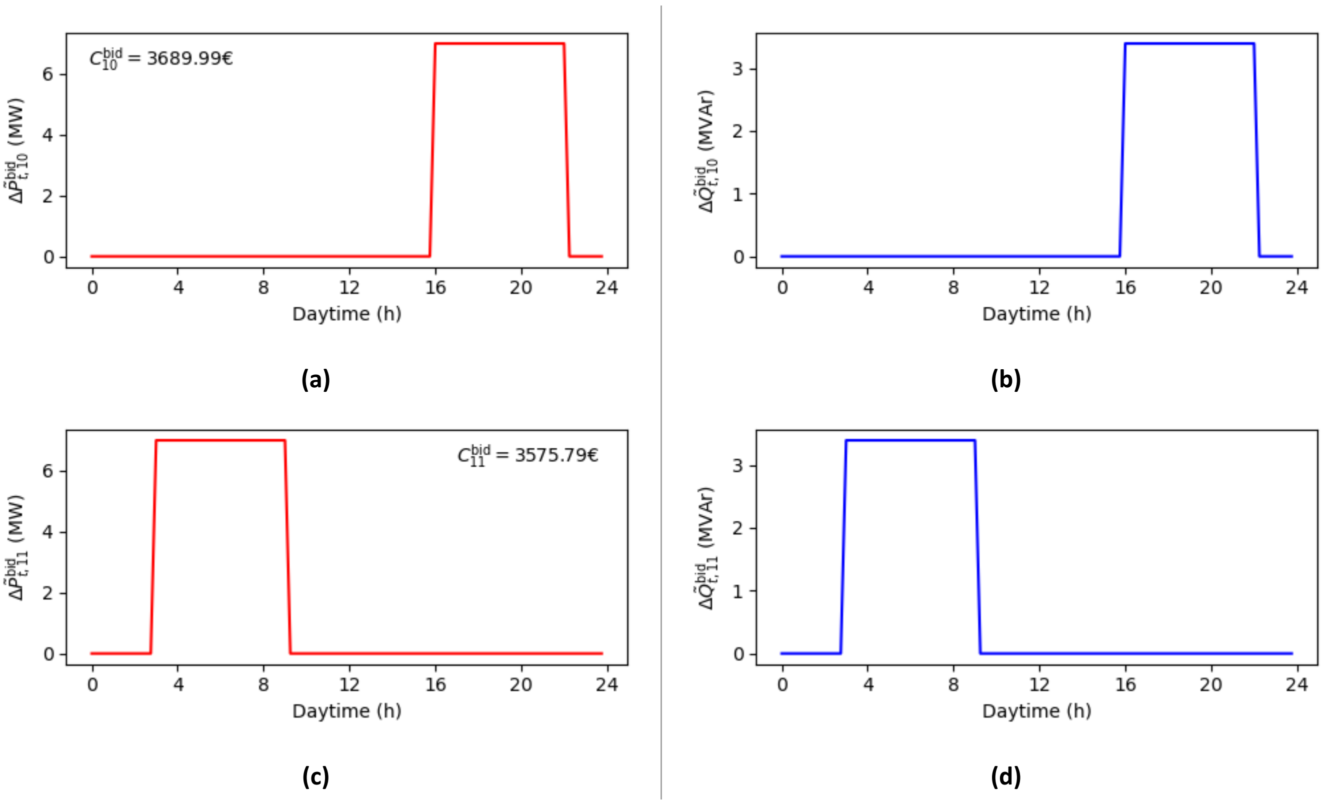

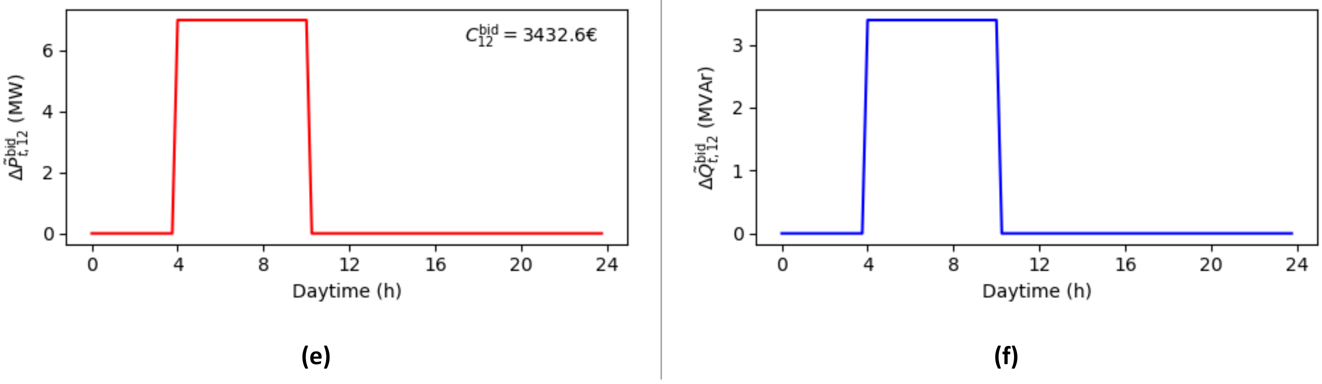

Figure 22: Bids and the associated direct reactive power changes of industry 'Ind_6': (a, b) Bid with ID 10; (c, d) Bid with ID 11; (e, f) Bid with ID 12.

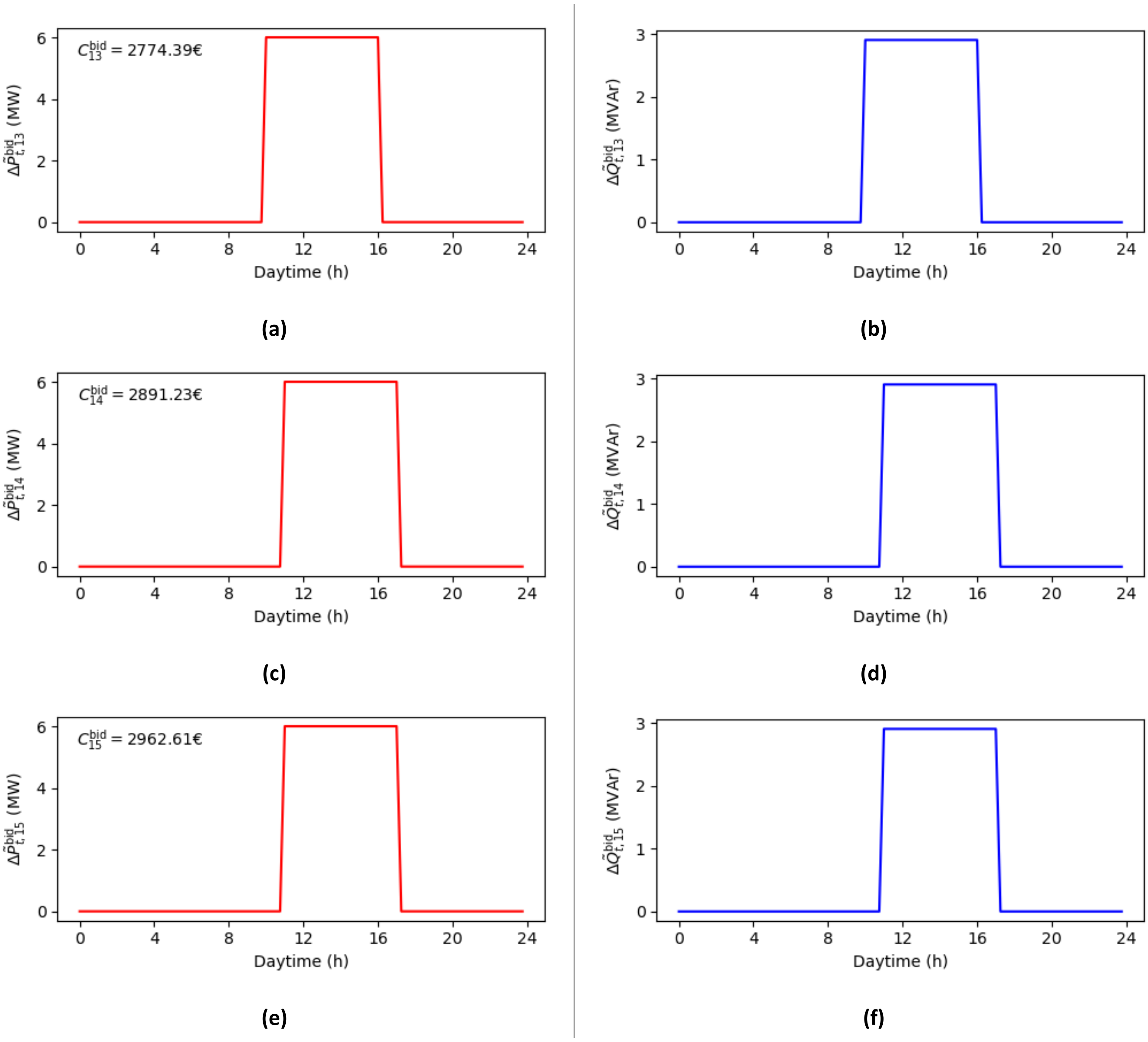

Figure 23: Bids and the associated direct reactive power changes of industry 'Ind_7': (a, b) Bid with ID 13; (c, d) Bid with ID 14; (e, f) Bid with ID 15.

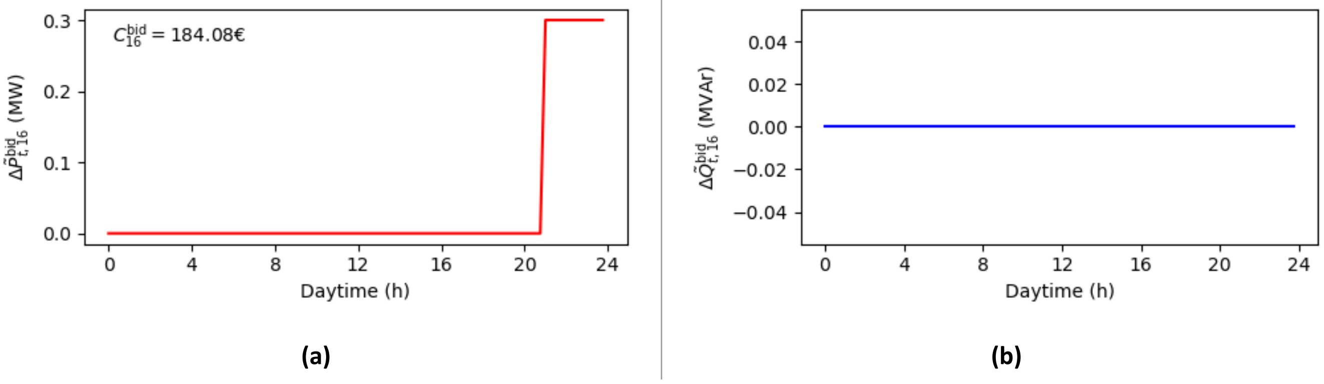

Figure 24: Bids and the associated direct reactive power changes of industry 'Ind_8': (a, b) Bid with ID 16.

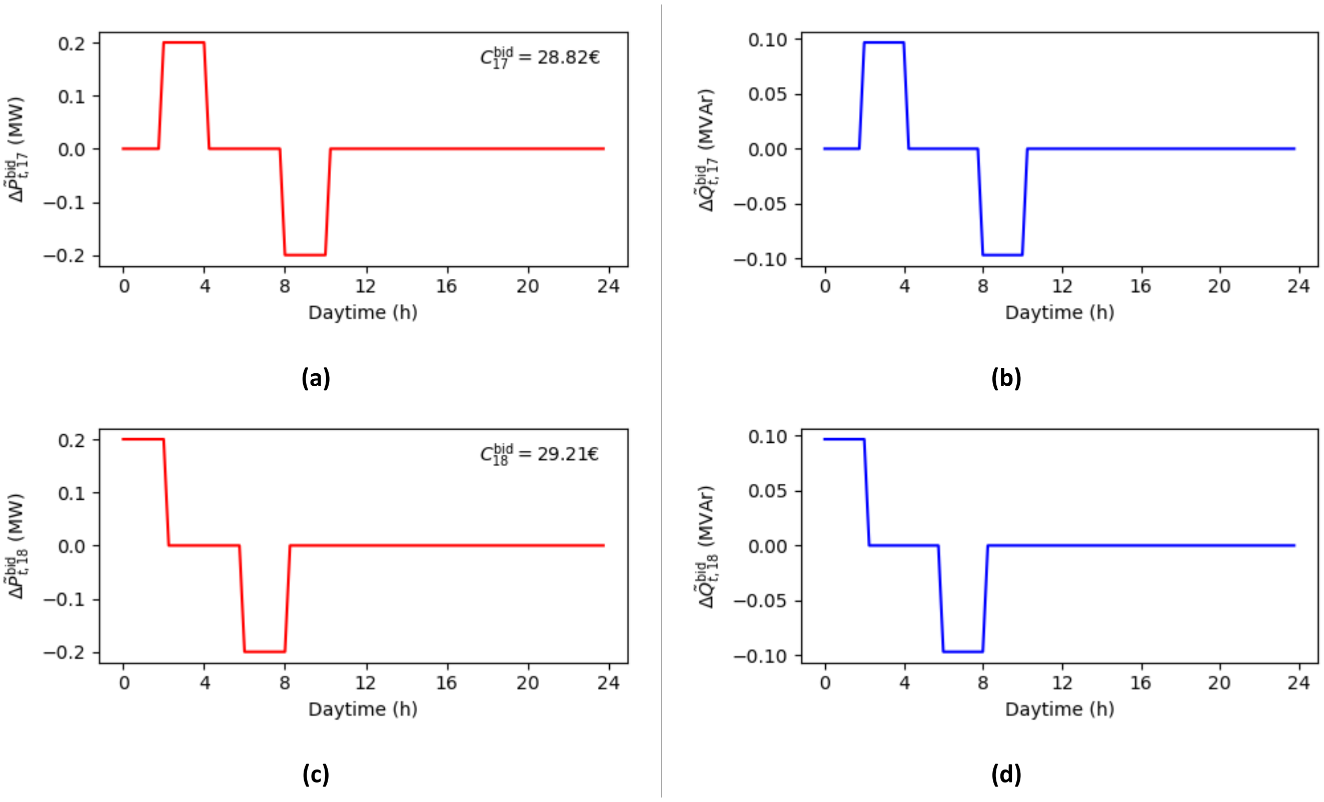

Figure 25: Bids and the associated direct reactive power changes of industry 'Ind_9': (a, b) Bid with ID 17; (c, d) Bid with ID 18.

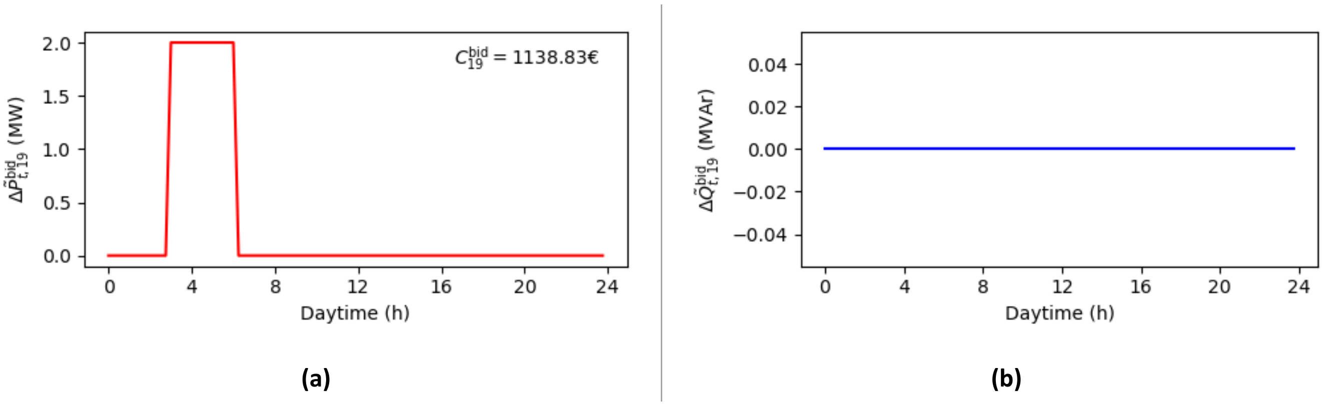

Figure 26: Bids and the associated direct reactive power changes of industry 'Ind_10': (a, b) Bid with ID 19.

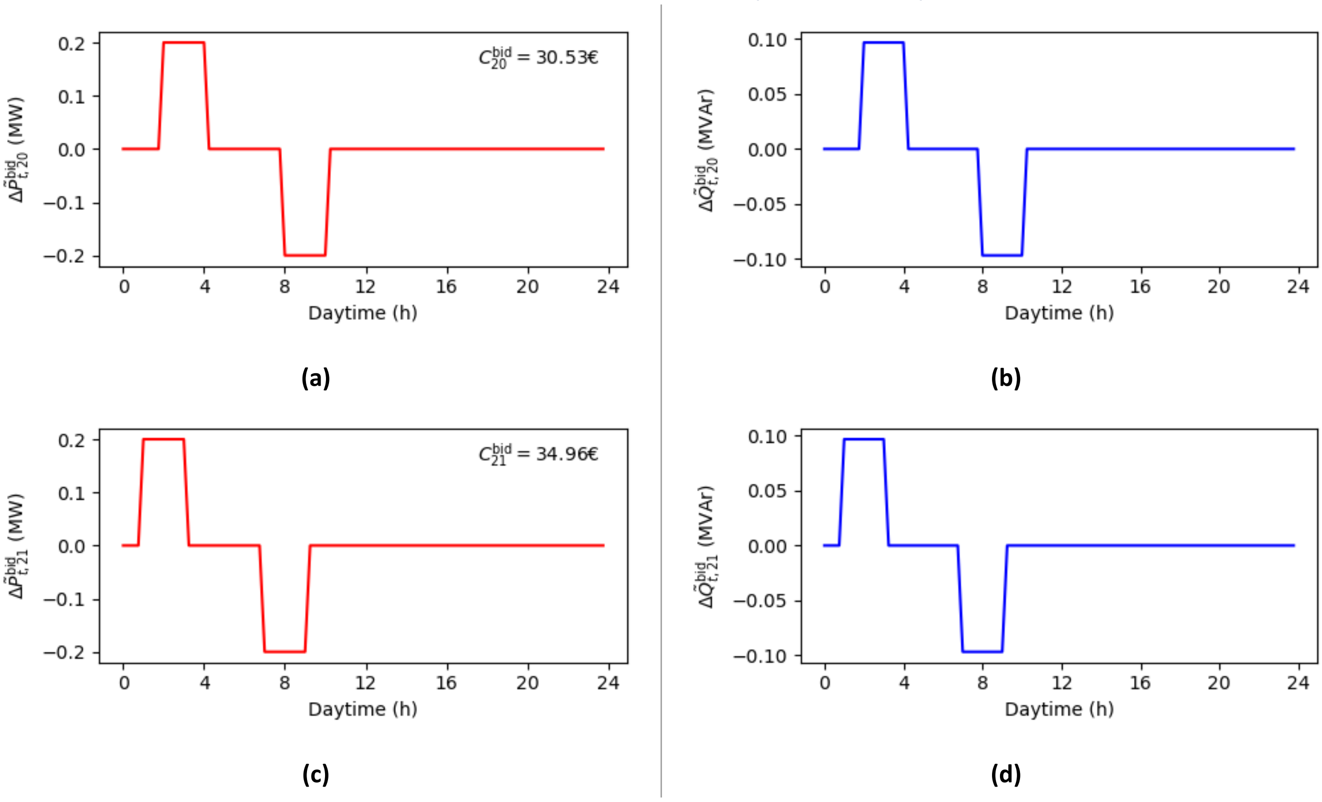

Figure 27: Bids and the associated direct reactive power changes of industry 'Ind_11': (a, b) Bid with ID 20; (c, d) Bid with ID 21.